MASTER PROJECT: FINAL REPORT

ENVIRONMENTAL SCIENCE AND ENGINEERING

The effects of urbanization on water quantity and quality in the Panke watershed, Berlin

EPFL Student:
Alma Vexina Wilkinson

EPFL professor:
Andrea Rinaldo , Laboratory of ecohydrology (ECHO)

Project Supervisor:
Paolo Benettin, Laboratory of ecohydrology (ECHO)

24 June 2022

Contents

Abstract

Constant growing urbanization worldwide which is known to affect the water cycle requires to develop new sustainable urban development plans. Although the effects of sealed surfaces in terms of water quantity for flood management are well known, little is known on the partitioning of specific rain events inside different urban configurations. Water age is a powerful tool which can help understand rainfall partitioning and water circulation inside an urban catchment. Here, an ecohydrological model and a virtual tracer input are used to trace specific summer and winter rainfall events through different typical urban parcels and quantify water age of significant output fluxes (surface runoff, evapotranspiration and leakage) through travel time distribution curves. Additionally, the effects of two urban development scenarios aiming at reducing surface runoff and increase water transit times inside each urban area were explored. The results show that the transit time of rainfall depends on rainfall partitioning which in turn is highly dependent on the type and amount of sealed surfaces present in the urban plot as well as the rainfall season. Winter rainfall has shown to have a greater transit time than summer rainfall because more water is flowing slowly out of the system through leakage. Also, only radical increases in permeable surfaces without vegetation have enough impact on rainfall partitioning to slow down transit times of water through the urban plots. These results form an important proof of concept on the use of water age to better understand the effects of different urban design strategies on the water cycle.

1 Introduction

Urbanization is growing steadily worldwide: by 2050, 68% of the world's population will be living in urban areas (United Nations, 2018). This transformation of the natural landscape into urban territory deeply modifies the different environmental cycles and interactions between them. Moreover, current urban areas are also transforming and forming new "city-territories" where the natural environment becomes intertwined with the urban realm. Thus, urban planners recognize there is a need to create new sustainable urban development strategies which aim at mitigating the environmental impacts of urban areas and ensure equilibrium between the natural and built environment, particularly regarding the water cycle. The Unites Nations also recognized this creation of sustainable urban areas needs to happen. They made it clear in their New Urban Agenda report (2016) where they declare a commitment to "long-term urban and territorial planning processes and spatial development practices that incorporate integrated water resources planning and management considering the urban-rural continuum". Furthermore, a special focus is drawn on "rehabilitating water resources within the urban [...] areas" by "minimizing water losses, promoting water reuse, increasing water storage, retention and recharge".
Urbanization affects the water cycle, with impacts on both water quantity and water quality. However, even if the effects of urbanization on water quantity related issues such as flood risk and drainage are well researched (Zhou et al., 2017), the effects of different urban configurations on ecohydrological partitioning, especially regarding evapotranspiration and groundwater recharge fluxes inside the urban landscape, are less explored (Kuhlemann, Tetzlaff, and Soulsby, 2020; Gillefalk et al., 2022). Moreover, there is a lack of knowledge on the effects of urbanization on water quality problematics in relation with solute transport. These unsolved problems call for new tools that can be used in a transdisciplinary context. One such tool may be the concept of water age, i.e. the time it takes for a raindrop to exit the catchment through runoff, evaporation or leakage to groundwater. Water age can be estimated using water stable isotopes acting as tracers and can give insights into water flux–storage interactions (Gillefalk et al., 2021). Indeed, tracking water through the urban landscape using water age can help discover its path which is relevant for assessing water partitioning inside an urban setting (Kuhlemann, Tetzlaff, and Soulsby, 2020). Furthermore, it can give insights into water quality as water age quantifies the time water spends in different compartments of the ecohydrological system and thus it represents the time available to interact with its surrounding environment.

1.1 Problem statement and objectives

A major remaining challenge is how to design an urban territory which ensures minimal impacts –and not just flood exposure– on the water cycle. This translates to the need to evaluate additional effects of different urban forms on the water cycle to be able to decide on the best urban development strategy for the future. Water age has the potential to give additional insights on water circulation in catchments and it may become useful to understand the effects of urbanization on the water cycle. Thus, the central research question of this project is: How do landcover changes affect water age in an urban catchment?
This master project is a part of a bigger interdisciplinary project: the Water Age Natural Habitats (WANH) project. It was a collaboration between scientists from two EPFL laboratories: Paolo Benettin from the Laboratory of Ecohydrology (ECHO) and Martina Barcelloni Corte and Cédric Wehrle from the Laboratory of Urbanism (Lab-U). Previous work of this project focused on the quantification of water fluxes and the long-term partitioning of precipitation into evapotranspiration, groundwater recharge and surface runoff inside different urban settings. This Master Project specifically focuses on the quantification of water age and the partitioning of individual rainfall periods inside the urban landscape.
To answer the central research question, the WANH project selected four different characteristic urban plots with different spatial configuration inside the Pankow neighborhood in Berlin: industry, single family housing, slabs and open blocks; and developed three different scenarios of urban development for each of the plots: the current scenario, a scenario implementing conservative landcover changes inside each urban plot and a scenario implementing more radical changes (see Methods section for an extensive description). This project therefore focuses on studying the impact of these urban design changes (i.e. changes in the landcover) aiming at reducing surface runoff and increasing water age inside each urban plot. Moreover, this project studies water age and partitioning of specific rainfall events occurring in summer and winter to have an overview of the impact of the landcover changes at different times of the year.

As mentioned before, the general goal of the project is to quantify the effects of different urban development scenarios on the water cycle by estimating water age. For this, an ecohydrological model able to

simulate tracer transport is used to run the simulations: the EcH_2O-iso model. In this context, virtual tracers are used to track specific rainfall events in two different seasons through each urban parcel for all the different scenarios. This will then allow to compute transit times and ecohydrological partitioning of rainfall water inside the different urban catchments for two critical periods of the year (summer and winter).
Thus, the more specific research questions of this project are:

1. What is the difference in ecohydrological partitioning and transit time of water for rainfall events in summer and winter in different urban settings?

2. What are the effects of permeable urban soils on the partitioning and transit time of rainfall water?

To answer the questions specific to this project, first, a review of the ecohydrological model used for the simulations is carried out. Indeed, a comprehensive understanding of the physical and hydrological processes which are modelled is imperative to correctly interpret results afterwards. Then, the model is run for the baseline simulations of each urban setting, meaning for the current situation. This creates a base to compare the urban parcels between them in their current state. Finally, the different scenarios are implemented for each urban setting and the corresponding simulations are run in order to assess to which extent urban design changes can have an impact on water partitioning, water age and solute transport.

1.2 Notations and Units used

- Notations
  - **WANH**: Water Age Neutral Habitats 'Project'
  - **DEM**: Digital Elevation Model
  - δ^2**H**: Deuterium isotope ratio. Deuterium is a stable water isotope. In this case in can therefore be used as a conservative tracer.

    The delta notation (δ) for isotopic composition quantifies, for a given water sample, the difference in the mass ratio of heavy to light isotopes (R) as compared to the Vienna Standard Mean Ocean Water (VSMOW): $\delta = (R_{sample}/R_{VSMOW} - 1) \cdot 10^3$.
  - **NMBTC**: Normalized Mass Tracer Breakthrough Curve
  - **TTD**: Travel Time Distribution
  - **ET**: The total evapotranspiration flux is the sum of three other subfluxes: the soil evaporation flux, the transpiration flux and the intercepted precipitation evaporation flux.
  - **Q**: Surface runoff flux.
  - **L**: Leakage flux. Also referred to as groundwater recharge flux.

- Units
  - **‰**: isotope ratio (permille)

2 Methods and Data

In this section, first, the method used to calculate the travel time distribution curves (i.e. water age o residence times computed at the time of exit) for the output fluxes considered in this project is explained. Second, the EcH$_2$O-iso model which is used to run the simulations is described as well as the way it is used to track specific rainfall events in the context of this project. Then, the method used for processing the results given by the model at the pixel level to get to the final fluxes averaged at the catchment scale is explained. Finally, the data used to run the simulations is described as well as the study areas which are the four different characteristic urban plots found inside the Pankow neighborhood in Berlin and the two scenarios of urban development which are studied.

2.1 Estimating water age using virtual tracer input

The goal of this project is to estimate water age (transit times) and partitioning of rainfall into the different considered output fluxes for the different urban plots under the different urban design scenarios. This is done by using virtual tracer applications coupled to a transport model. Indeed, quantifying water fluxes and storage dynamics coupled to tracer transport can provide important insights into water pathways.
However, while water fluxes are controlled by celerities (how fast energy propagates via the hydraulic gradient), solute transport depends on the actual velocities of molecules along hydrologic pathways (how fast water parcels move) which results in radically different travel times (McDonnell and Beven, 2014). And, it is tracers which allow to highlight the pore velocity of water molecules (Kuppel et al., 2018).
Therefore, in this project, a virtual isotope concentration (or isotope signature) in the different hydrological compartments (storages and fluxes) is used to track rainfall through the urban hydrological system. The timeseries of isotope concentration in precipitation which must be supplied to the model as an input, in this case, corresponds to the timeseries of input of the virtual tracer in precipitation water instead of the 'normal' meteorological timeseries of isotopes in precipitation water (see 2.4.1 for more details).

For this project, summer and winter are selected as the periods of the year to analyse water pathways to have a comparison of rainfall water partitioning and transit time for two complete opposite seasons and therefore conditions. Thus, the selected periods of precipitation to track are December 2017 and June 2018. Indeed, December 2017 represents winter rainfall and June 2018 represents summer rainfall. It is important to notice that the rainfall events to be tracked are chosen within the first year of the simulation period so it is possible to follow the water the longest time possible through the urban landscape in the simulations results as only 2 complete years of data (30.11.2017-30.11.2019) are available for the analysis period (see complete description in 2.4.1).
Figure 1 shows the periods of rainfall that are tracked in different simulations which therefore also represent the periods where there is an input of the virtual tracer which is one month long each time.

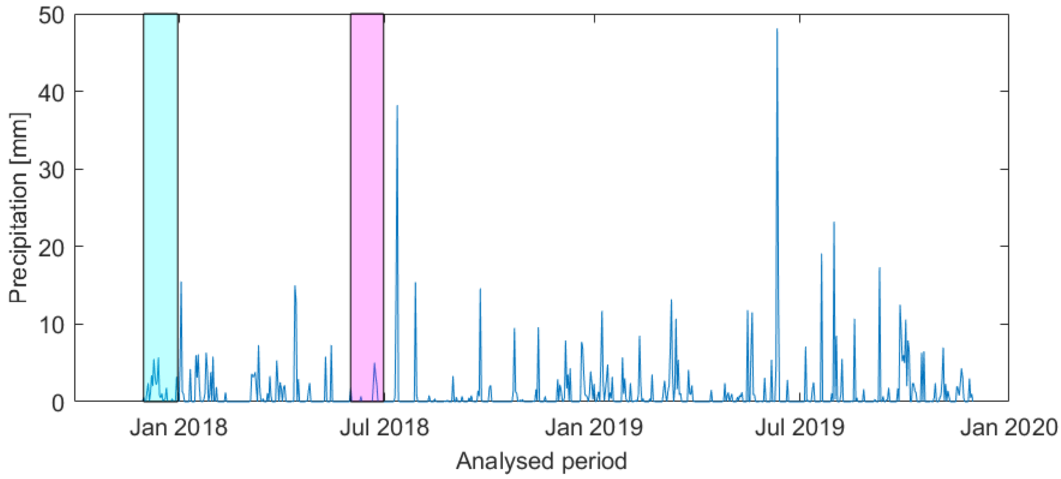

Figure 1: Precipitation timeseries with highlighted periods of virtual tracer input, blue for the winter rainfall (December 2017) and pink for the summer rainfall (June 2018)

Water age is estimated in this project by computing the travel time distribution (TTD) of winter and summer rainfall. Therefore, each characteristic urban plot and scenario is characterized by a winter and summer TTD. As in this case the stable isotopes act as a tracer, computing the TTD curves for the output fluxes as an approach to water age enables the understanding of tracer transport in the urban landscape by showing the velocity of water for the different fluxes.
The TTD (p_F) represents the normalized mass breakthrough curve ($NMBTC_F$) of a perfect tracer for a specific flux F. It quantifies the lag times at which an instantaneous precipitation input is released to F. Measured tracer data or tracer simulations obtained using a transport model (such as in this project) can conveniently give the concentration breakthrough curves (CBTC) of a specific flux for each tracer application. Therefore, the CBTC must be then be multiplied by the specific flux (F) to obtain the mass breakthrough curve of said flux:

$$MBTC_F = CBTC_F \cdot F; \tag{1}$$

Finally, the $MBTC_F$ must be normalized by the total mass of tracer input applied during the application period (M_0) to get the normalized MBTC of the individual fluxes ($NMBTC_F$). It is important to note that in this project, the obtained NMBTC of the individual fluxes do not sum to 1 because not all the applied tracer mass goes to each particular flux. Indeed, the integral of the NMBTC (i.e. the cumulative $NMBTC_F$) of a particular flux reflects which fraction of the applied tracer mass goes into that particular flux (θ_F).
Therefore, to finally obtain a TTD for a particular flux, the NMBTC must be normalized by the NMBTC area. Indeed, the TTD curve represents the mass of tracer recovered at each timestep by an output flux compared to the total tracer mass which is recovered by the same output flux at the end of the analysis period.
Equation 2 thus shows the computation of the TTD from the $MBTC_F$:

$$p_F = NMBTC_F = \frac{MBTC_F}{\theta_F \, M_0}; \tag{2}$$

Finally, it is important to note that this project focuses on computing TTDs at the catchment scale or in this case at the urban plot scale and not at the pixel level. Therefore, measured data or data obtained as results of a spatially-distributed model should give the tracer concentration in each flux of interest averaged at catchment scale as well as the value of each of the fluxes averaged at the catchment scale.

2.2 EcH$_2$O-iso model

To compute the travel time distribution curves and get the transit time of rainfall and its partitioning inside the different urban plots and for the different urban development scenarios, a model which gives as result the timeseries of fluxes averaged at catchment scale as well as timeseries of the virtual tracer concentration for each flux averaged at catchment scale is needed. Thus, the EcH$_2$O-iso model described in this section was chosen at the beginning of the WANH project.

2.2.1 General description

EcH$_2$O is a spatially distributed, process based ecohydrological model developed by Maneta and Silverman, 2013. It couples a vertical energy balance scheme module solved at soil level and canopy level, with a water balance module which computes vertical and lateral water transfers (using the Green-Ampt equation to calculate infiltration and a 1D kinematic wave approach based on the steepest slope approach for subsurface flows), and with a vegetation growth module which is based on the calculation of gross primary production. The three modules are coupled explicitly in order to capture all feedback and interactions between these three modules at an hourly to daily timescale and adequately represent the soil–plant–atmosphere continuum.
The model uses hydroclimate data as input data. It can come from the outputs of regional climate models or it can be actual real measured data (as in this project). This means precipitation, incoming longwave and solar radiation, air temperature (Tmax, Tavg and Tmin), relative humidity and wind speed timeseries for Berlin are needed in this project. Furthermore, as the model is spatially explicit it also requires a landcover map of the modelled area and a digital elevation model (DEM) to define the topography and the drainage network of said area. Finally, the model needs a file specifying the distribution of the different vegetation species inside the modelled area.

Kuppel et al., 2018 further developed this base ecohydrological model to include an isotope tracking module thus creating the EcH_2O-iso model. This new module does not require site specific calibration for new parameters and allows to track naturally present water stable isotopes: ^2H and ^{18}O inside a catchment.
It models conservative tracer transport by computing transformations in the isotope composition of water as it flows through the ecohydrological system and evaporative fractionation and mixing processes occur. Indeed, the module allows for isotopic fractionation to be taken into account for soil water evaporation and evaporation of intercepted precipitation if desired. However, fractionation in the transpiration flux isn't implemented in the model. Furthermore, all calculations are based on the assumption of instantaneous and complete mixing at each timestep in each hydrological compartment (hydrological storages and fluxes) such that the resulting isotope signature given by the isotope tracking module relates to the bulk composition of water in each hydrological compartment.
Moreover, the isotope tracking module also computes the mean water age in each modelled compartment/flux by increasing the age of the water at the end of each timestep by the length of said timestep while taking into account that precipitation has an age of zero. Indeed, in the case of these water age computations, the assumption of complete mixing also applies for all hydrological compartments.
The EcH_2O-iso model therefore uses the following mass balance equation (eq. 3), taking into account the instantaneous complete mixing assumption, to compute the resulting water signature for each hydrological compartment:

$$\frac{d(V_{res}C_{res})}{dt} = \sum_{k=1}^{N_{in}} q_{in,k}C_{in,k} - q_{out}C_{res} \tag{3}$$

where V_{res} and C_{res} are, respectively, the volume and signature (δ^2H, $\delta^{18}O$, or age) of the water in the reservoir, t is time, q_{out} is the flux of water exiting the reservoir, and $q_{in,k}$ and $C_{in,k}$ are, respectively, the flux and signature of water entering the reservoir from each the N_{in} adjacent upstream locations (Kuppel et al., 2018).

The main reason why the EcH_2O-iso model is chosen for this project is because it allows to track precipitation events through the modelled landscape/catchment. Indeed, one can use the water signature in each hydrological compartment or flux and combine it with the volume of said compartment/flux to track the rainwater and estimate its travel time distribution as is explained in Section 2.1.
It is also important to highlight that the key point to correctly simulate water pathways is that it is imperative to correctly model the duality between velocity fields (how fast the water parcel moves) and the celerity of water (how fast energy propagates according to the hydraulic gradient). And, the EcH_2O-iso is proven to reasonably capture the velocity fields with consistent tracer concentrations at given locations and points in time across the catchment in addition to simulating well the catchment functioning from a celerity viewpoint (Kuppel et al., 2018).
Nonetheless, even if the model is proven to correctly simulate water velocities and celerity, the results depend heavily on the quality of the inputs of the model. Indeed, simulating the correct isotope dynamics is conditioned by the correct calculation of water particle velocities patterns which in turn depends on having the correct routing of the water parcels from the precipitation site to their output location. This means that the DEM is a crucial input of the model which determines its accuracy regarding water pathways and velocities. Thus, in order to have a correct data set on which the modelling can be based on, prior to this project, a whole analysis of the DEM of each modelled urban plot is needed (work carried out in a previous SIE project by Camille Dross).
Moreover, the EcH_2O-iso model has some limitations given the processes it takes into account in each module. Indeed, the base model does not take into account diffusion processes and does not have an explicit biogeochemical cycle for ecosystem respiration. Moreover, when the model uses the isotope tracking module, the dynamic allocation for vegetation is not activated. This means the biomass allocated to the different parts of each plant does not vary with the seasons and stays equal to the initial condition. Finally, there are not lateral input and output fluxes connecting the pixels laterally in the first soil layers. Despite these limitations, EcH_2O-iso was already used in various studies and yielded satisfactory results and insights both for its basic format and using the isotope tracking module for different climate conditions and different research topics (see Maneta and Silverman, 2013; Kuppel et al., 2018; Gillefalk et al., 2022). Furthermore, the recent work of Gillefalk et al., 2021 using the EcH_2O-iso model is particularly interesting as they tested the complete version of the model (with the isotope tracking module) for a watershed located in Berlin, Germany. The studied area was an urban plot and they focused on 3 types of landcover with vegetation: grass, shrub and trees. Their results show that the model, once the parameters are

calibrated, adequately predicts isotope signature of water at the different water depths as well as the soil water content and thus the simulations give overall realistic results. Indeed, it is important to notice that Berlin has very good draining soils meaning that the fact that no lateral exchanges in the first soil layers are included in the model does not misrepresent the reality of the modeled catchment.
Thus, EcH$_2$O-iso model is a good choice for this project. Indeed, it is already well tested and proven to give accurate results and there is an existing list of calibrated and validated parameters for the Berlin region (created by Gillefalk et al., 2021) which can be reused for this project given that the parameters in the isotope tracking module do not require site specific calibration.

2.2.2 Details of the EcH$_2$O-iso model use in this project

The EcH$_2$O-iso model integrates a high number of fluxes which connect the different hydrological storages between them. Indeed, as can be seen in Figure 2, the model integrates components for the storage of intercepted precipitation by vegetation species, the storage of snow and ponding water on the soil's surface. Furthermore, the sub-surface is divided into 3 different compartments as the soil is split into a topsoil layer, an intermediate soil layer and a deep soil layer with the groundwater storage component of the model being a part of this third soil layer too. Finally, the model enables the possibility to integrate a stream as a separated hydrological compartment which has its own storage and relates exclusively to the ponding water and to groundwater components. Finally, Therefore, the model is overall quite complete in its modelisation of the hydrological system.

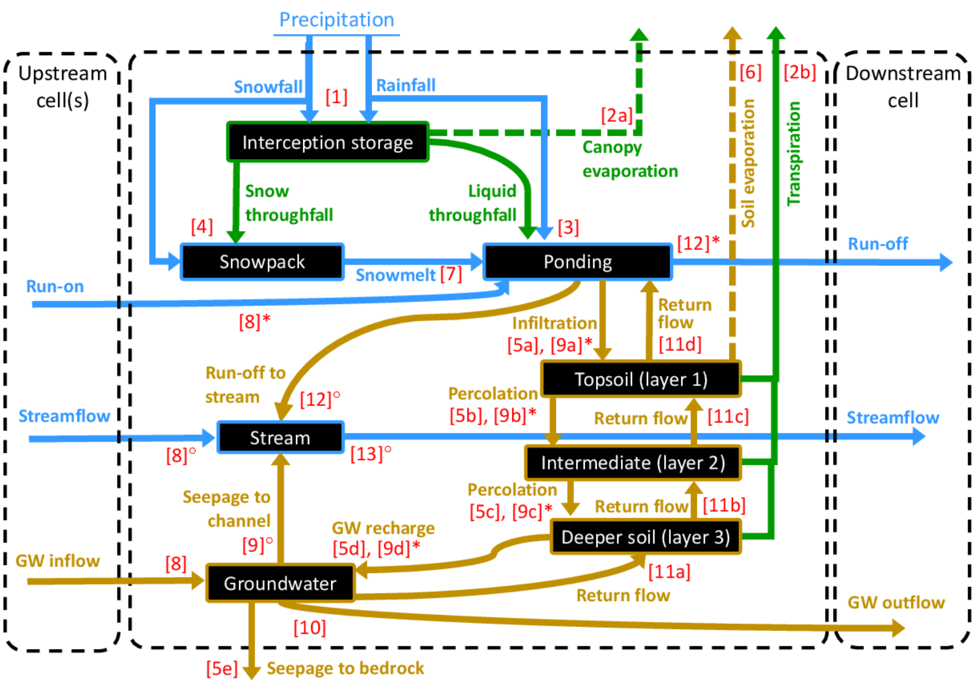

Figure 2: Hydrological storages and fluxes computed in the hydrological module in EcH$_2$O-iso (at the pixel level). Source: Kuppel et al., 2018.

However, the model also includes an option to activate or deactivate several processes using binary switches in the configuration files of a simulation. This characteristic of the model is used in this project to only activate the processes which are of use to model the path of a conservative tracer present in rainfall as realistically as possible in a urban catchment.
Indeed, one of the existing options enables water which runoffs from a given cell to re-infiltrate in a downstream cell. This option is deactivated for this project in order to simulate the runoff of rainwater directly into the drainage network as the latter can not be explicitly integrated into the model.
Furthermore, as explained before, the isotope tracking module includes the possibility to include isotope fractionation for certain fluxes of the hydrological system. However, as the water stable isotopes are used as virtual tracers in this project to track specific rainfall events in each urban plot by recognizing the signature of the marked rainwater in the different hydrological compartments of the system through

time, all isotope fractionation is deactivated (i.e. fractionation for the soil evaporation flux and for the evaporation of intercepted precipitation).
Finally, in this project, there no streams flowing trough the urban catchments which are modelled. Therefore, this option is also deactivated.

Moreover, EcH$_2$O-iso gives the possibility to track two different water stable isotopes but deuterium (δ^2H) is the only isotope which is used in the simulations.

The goal of this project is to analyse the partitioning of rainfall and its transit time in the urban landscape. Therefore, only certain fluxes computed by the EcH$_2$O-iso model are used for the research. Indeed, the focus is on the main output fluxes of the system and precipitation as the only input flux. Figure 3 shows the hydrological system considered for this project. As can be seen, the deepest soil layer is left out of the hydrological system which means that leakage or percolation of water from the second soil layer to the third soil layer is considered as groundwater recharge, one of three output fluxes. Moreover, evapotranspiration, which is the sum of the soil evaporation, transpiration and intercepted rain evaporation fluxes computed by the model, is considered as the second output flux of the system. Finally, surface runoff is considered the third output flux of the system.

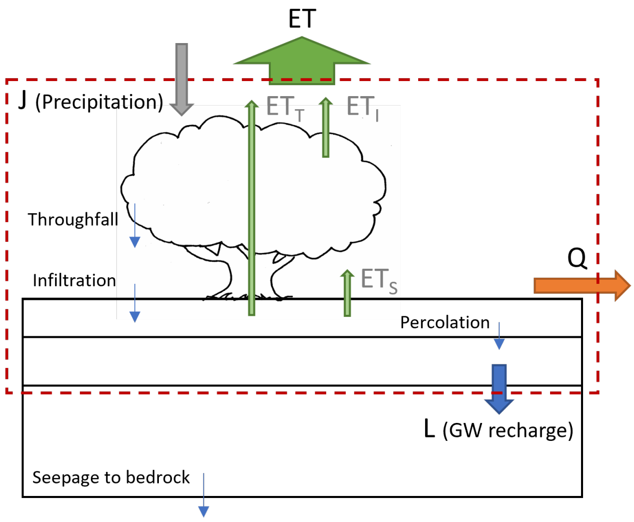

Figure 3: The simplified system which is analysed within the broad EcH$_2$O-iso model is delimited by the red rectangle. The output fluxes which are taken into account in the hydrological balance are represented with full arrows in orange (surface runoff), green (total evapotranspiration) and blue (leakage or groundwater recharge).

The resulting overall mass balance equation therefore used in this project for the analysis at catchment scale is shown below (eq. 4), with Q as the surface run-off, ET as the evapotranspiration and L as the groundwater recharge (or leakage) and J as precipitation. S refers to the amount of water stored inside the soil and M to the mass of isotope stored in the soil. The notation δD_x refers to the concentration of deuterium in the flux or storage x.

$$\frac{dM}{dt} = \frac{d(S\,\delta D_S)}{dt} = J\,\delta D_J - ET\,\delta D_{ET} - L\,\delta D_L - Q\,\delta D_Q \tag{4}$$

Many simulations are launched to analyse the behavior of rainfall water in different urban configurations. Indeed, the objective is to have a comparison of rainfall partitioning and transit times between different seasons in different urban parcels and with different plausible scenarios of urban development. Since there are 4 different urban fabric types studied (Industry, Slabs, Open Blocks, Single Family Housing), 3 scenarios of urban development (current situation, conservative changes and radical changes) and 2 seasons (summer and winter), there is a total of 24 simulations to run at a daily timescale at a 1m resolution on urban parcels which have a 250mm surface each.
Given the quantity of simulations to run in this project, a python script which automatically generates all the folders with the correct input files to run each simulation with the model is created. The data files, initial conditions and parameters that must be specified as inputs for the model to run the simulations are explained in section 2.4.1.

2.3 Results processing method

As mentioned in Section 2.1, the timeseries of the different fluxes considered in the mass balance and their respective isotope signature averaged at the catchment scale are needed for the computations of the travel time distribution curves.
Fortunately, the EcH_2O-iso model is able to produce as output a file with all the timeseries of the different fluxes studied already averaged at the catchment scale. Moreover, normally, a similar output file should be produced with the timeseries of the isotope signature of each flux averaged at the catchment scale.
However, there is an error in the computations of the summary file containing the isotope signature of each flux. Indeed, there seems to be a problem with the fact that some of the landcovers present in the modelled areas of this project have no vegetation on them as the project analyses urban landscapes. In fact, the pixels covered with asphalt, building, pavement or gravel, have some fluxes such as the evaporation of intercepted water by vegetation and the transpiration of vegetation which are zero. This creates a problem in the computations of the isotope composition of said fluxes averaged at catchment scale as a division by zero takes place. Thus, the results for the isotope signature of these fluxes averaged at catchment scale end up being NAN values at each timestep in the summary file. This means that the timeseries of isotope signature of the total evapotranspiration flux (ET flux) also ends up being filled with NAN values in the summary file as the ET flux is the sum of the soil evaporation flux, the transpiration flux and the intercepted precipitation evaporation flux and its isotope signature is the weighted average of the isotope signatures of the sub-fluxes and the value of each of these fluxes.
Therefore, the model gives the timeseries of all input and output fluxes considered in the hydrological system of this project averaged at catchment scale and ready to be used to calculate travel time distributions. Furthermore, the model gives the correct output timeseries of isotope signature averaged at catchment scale for precipitation, surface runoff and leakage. However, the isotope signature of the evapotranspiration (ET) flux averaged at catchment scale is not correctly calculated and is therefore the only timeseries missing from the model outputs for the computation of all travel time distribution curves of interest for this project.

Various solutions to obtain the missing timeseries for the isotope signature of the evapotranspiration flux averaged at the catchment scale were explored during this project.
On the one hand, it was tried to solve the problem by modifying the part of source code of the model computing this timeseries but it was not easy at all (even with the help of the model developers) and therefore after a few failed attempts this idea was let go.
On the other hand, it was thought of using the different maps which can be generated by the model (as it is spatially explicit) for each timestep of the simulation containing the value of each of the subfluxes composing the total ET flux and their isotope signature. The idea was to compute the weighted average of all the maps mentioned before and create a new map containing the isotope signature of the overall ET flux to then aggregate all pixels and obtain the isotope signature of the ET flux averaged at the catchment scale. However, this type of calculations would have been too expensive computationally so this second solution was not pursued either.
Therefore, a third solution which uses another already existing output of the model was adopted to compute the missing timeseries. Indeed, the model has an interesting existing feature which allows to place virtual probes at chosen locations inside the catchment (in certain pixels of the modelled area). Furthermore, it gives the possibility to have as an output a timeseries for chosen variables such as the value of the different subfluxes composing the total ET flux and their respective isotope signature at each location were a probe is placed. This means that strategic probe locations can be chosen inside each modelled urban plot such that the output timeseries can then be aggregated to obtain the final timeseries of isotope signature of the evapotranspiration flux averaged at catchment scale following the algorithm described in the next paragraph. It is important to notice that in order to have an accurate estimation of the average isotope signature of the ET flux at the catchment scale using this method, a subset of pixels which is representative of the overall modelled area has to be chosen to put the probes in as it is not possible computationally to integrate the results from probes in all pixels in the calculations. Therefore, as fluxes are not homogeneous spatially, various probes have to be placed in pixels having the same landcover type to obtain a mean of each flux and its associated isotope signature for a given landcover type even if for the ET flux, the flux value seems to be pretty constant for one same landcover type throughout a given urban fabric type. This results in between two and six probes being placed on pixels corresponding to each landcover type (asphalt, building, gravel, pavement, grass, shrub, trees and vegetated roof) in each modelled catchment (each urban fabric type and respective scenarios).

The algorithm used to aggregate the probes timeseries together and get the final timeseries of isotope signature of the ET flux averaged at catchment scale is shown below (Algorithm 1) and works as follows. Firstly, the average of the isotope signature and value of each subflux composing the ET flux (soil evaporation, intercepted precipitation evaporation and transpiration) for each type of landcover found inside each modelled catchment is calculated. Then, the weighted average between the average value, respectively the isotope signature, of each subflux for each landcover type and the proportion of each landcover type inside each modelled area is computed to obtain the average flux value, respectively the isotope signature, of each component of the ET flux at the catchment scale. Finally, the weighted average between the last two computed terms, meaning the average value of each subflux at catchment scale and their respective isotope signature, is calculated to obtain the overall average isotope signature of the ET flux at the catchment scale.

Algorithm 1: Calculating $\delta^2 H(ET)$

for flux ET_x in flux_ET **do**
$Tp \leftarrow$ timeseries of evapotranspiration flux component in each probe location (in m/s)
$Tp \leftarrow Tp \times 1000 \times 24 \times 3600/pixelarea$ (Fluxes are now in mm)
$Tp\_iso \leftarrow$ timeseries of isotope signature of evapotranspiration flux component in each probe location (in ‰)
$f_{LC} \leftarrow$ fraction of each landcover in the catchment

{– Average of flux and isotope signature for each ET flux component in each landcover –}

for LC in LC_list **do**
$(ET_x)_{LC} = (\sum_{probe=1}^{n^o probesLC} (ET_x)_{probe})/n^o probesLC$
$\delta^2 H(ET_x)_{LC} = (\sum_{probe=1}^{n^o probesLC} \delta^2 H(ET_x)_{probe}))/n^o probesLC$
end for

{– Weighted average of flux and isotope signature for each ET flux component over the whole catchment –}

$ET_x = \sum_{LC=1}^{n^o LC} (ET_x)_{LC} \times f_{LC}$
$\delta^2 H(ET_x) = (\sum_{LC=1}^{n^o LC} \delta^2 H(ET_x)_{LC} \times (ET_x)_{LC} \times f_{LC})/ET_x$

end for

{– Weighted average of flux and isotope signature for the overall ET flux over the whole catchment –}

$ET = \sum_{x=1}^{n^o ETcomponents} ET_x$
$\delta^2 H(ET) = (\sum_{x=1}^{n^o ETcomponents} \delta^2 H(ET_x) \times ET_x)/ET$

The accuracy of the results given by the algorithm was verified by simulating a test catchment (5x5 pixels) covered exclusively in vegetated landcovers with a tracer input in rainfall during the whole month of December 2017. Indeed, a comparison of the NBMTC curves and cumulative NMBTC curves obtained following the overall method explained in section 2.1 and the different outputs of the model was done. The plots showing the results of this comparison are presented in Figures A1 and A2.
Firstly, the NMBTC and cumulative NMBTC curves were calculated by using the timeseries given by the output summary of the model for the value of the ET flux averaged at catchment scale and its isotope signature. Secondly, they were calculated by using the timeseries given by the output summary of the model for the value of the ET flux averaged at catchment scale and the timeseries ET flux averaged at catchment scale calculated using the algorithm.
The results obtained by using the algorithm were satisfactory as the NMBTC calculated using the timeseries of isotope signature of the ET flux averaged at catchment scale given by the algorithm is almost identical to the NMBTC calculated using exclusively the timeseries given as outputs of the model. Furthermore, the cumulative NMBTC also shows that the final amount of isotope mass recovered by the ET flux is almost identical in both cases (only 1.5% difference) meaning that the timeseries of isotope sig-

nature of the ET flux averaged at catchment scale calculated by the algorithm has an acceptable accuracy.

Therefore, in this project, the timeseries of isotope signature of the total evapotranspiration flux averaged at the catchment scale is calculated using this algorithm and is then combined with the timeseries of the value of the evapotranspiration flux averaged at catchment scale given as an output of the model to compute the travel time distribution of the evapotranspiration flux for each modelled urban plot using the method explained in section 2.1.

2.4 Data

2.4.1 Meteorological data, initial conditions, parameters

As mentioned before, the EcH_2O-iso model uses as main inputs timeseries of precipitation, incoming longwave and solar radiation, air temperature, relative humidity and wind speed.
Collaboration between ECHO laboratory at EPFL and the IGB institute in Berlin allowed the access to the measured hydroclimate data for the Berlin region. Thus, 2 years and 3 months of original data were available: from the 1^{st} of March 2017 to the 30^{th} November 2019. This original data is at an hourly resolution, but the simulations of this project run at a daily timescale. Thus, as a first step, it was necessary to compute the timeseries at a daily resolution. Furthermore, 2 complete years of data were desired for the analysis period while having one entire year of spin-up period beforehand. Thus, the timeseries with the original data was completed such as to have 3 complete years of hydroclimate data at a daily resolution for the simulations. For this, the data from December 2017 to February 2018 was copied to the beginning of the timeseries to have 3 complete years of data as shown in 4 for the example of the precipitation timeseries.
The isotope tracking module also requires the timeseries of isotope concentration in precipitation as input. Normally, measured or modelled data of the values of isotope concentration in precipitation would be used. However, in this project, the isotopic composition of water acts a tracer which is used to track specific chosen rainfall events as explained before (see section 2.1). Thus, two sets of timeseries for the deuterium isotope concentration in precipitation are manually generated for the two different seasons of tracer input. These isotope timeseries are built the following way for the different simulations: the isotope concentration in precipitation is 0‰ during all the simulation except during the period of rainfall to be tracked where the isotope concentration has an arbitrary value of -60‰. Therefore, the simulations tracking summer rainfall use as input timeseries for the isotope concentration in precipitation a timeseries built such that the concentration is -60‰ from the 1^{st} of June 2018 to the 30^{th} of June and the rest of the days the concentration is 0‰. Instead, the simulations tracking winter rainfall use as input timeseries for the isotope concentration in precipitation a timeseries built such that for all days the concentration is of 0‰ except from the 1^{st} of December 2017 to the 31^{st} of December were the concentration is of -60‰. These input timeseries for the isotope concentration in precipitation also have a daily resolution and are 3 years long.

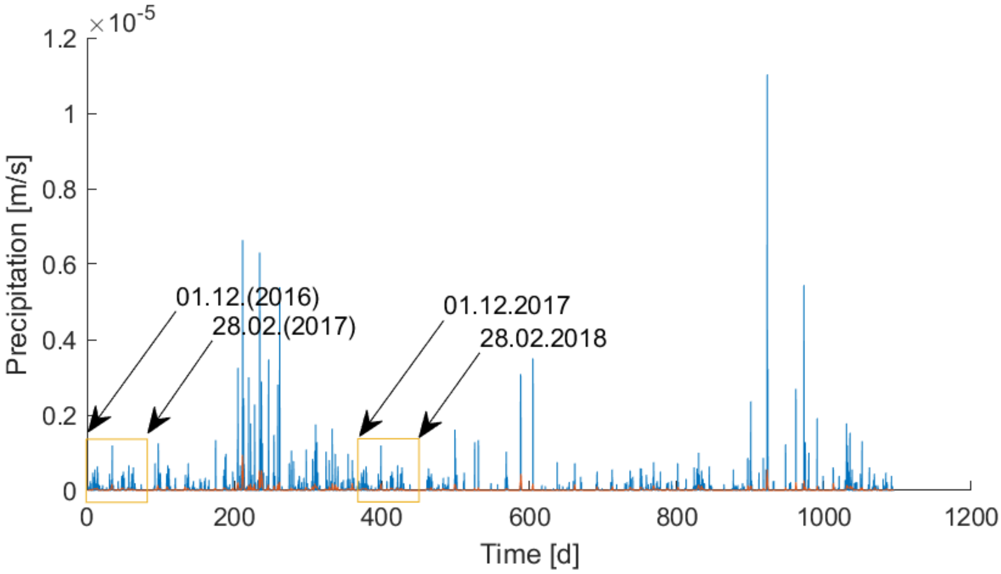

Figure 4: Precipitation timeseries used for the simulations at a daily resolution (in red) compared to the original precipitation data at hourly resolution (in blue). The periods of 'copied' data are highlighted in orange.

Moreover, the model requires some initial conditions to be able to compute the different hydrological fluxes and storages as well as the energy fluxes and the growth of the vegetation species during the simulation. Indeed, the soil moisture, soil temperature, snow water equivalent present on the ground are needed. These are set assuming that the catchment starts free of snow, with 50% of the pores saturated with water and with a temperature of 10°C throughout the catchment. Furthermore, the initial values of isotope concentration in the different hydrological compartments are needed to be specified as maps as inputs of the model. These are set to zero over the whole catchment in all the hydrological compartments so as to have no background tracer concentration in water and easily identify the marked rainwater. Finally, various initial conditions are needed for vegetation. There are 4 different vegetation patches in this case study: bare soil (all landcovers without vegetation species), grass, shrubs and trees which are made of different proportions in species. The grass patch is made of 10% trees, 80% grass and 10% bare soil; the shrubs patch is made of 10% grass, 60% shrubs and 30% bare soil; and the trees patch is made of 60% trees, 20% grass and 20% bare soil. For all these patches with vegetation, the stem density, the root density, the stand age, the leaf area index (LAI), the effective height and the total stand basal area are specified for each species as initial conditions in the inputs of the model.
Finally, the model also requires some parameters which must be calibrated and validated to run the simulations and get accurate results. They can be separated into 'soil parameters' and 'vegetation species parameters'. For this project, no calibration of parameters is done. Indeed, all soil parameters for the landcovers with vegetation (grass, shrub and trees) and the parameters for these three vegetation species used in the simulations are taken from Gillefalk et al., 2021 since they have created a set of validated parameters for the region of Berlin. The soil parameters for the other landcovers (asphalt, building, gravel, pavement and vegetated roof) were estimated from literature at the beginning of the WANH project. Table A1 lists all the soil parameters that are used in the simulations.

2.4.2 Urban fabric types

In this project there are four different urban plots which are studied as independent "catchments". They reflect four different types of urban structures with unique characteristics and are therefore considered to be different urban fabric types (UFT). Indeed, each urban parcel is composed of different proportions of specific landcovers laid out in a particular way. There are eight landcovers which compose each urban fabric type. There are four landcovers without vegetation: asphalt which is mostly used for the roads, building which corresponds to all the roofs of houses and buildings, pavement which is used for some roads and walkways and is made of cobblestones, and gravel which is mostly found in some unused spaces of the different urban plots and around buildings. And there are also four vegetated landcovers: grass, shrubs, trees and vegetated roof which is in reality a fictive landcover created for the urban development scenario implementing radical changes. Indeed, only the 7 first mentioned landcovers compose the different urban fabric types in the current situation.

The four different urban plots which are studied in this project are illustrated in Figure 5. They are all located close to another in the Pankow neighborhood in Berlin as can be seen on the map. To be able to compare the results between the different urban landscapes, each studied parcel has a surface of 250mx250m. Thus, the areas which are modelled do not represent real catchments but squares of typical urban fabric types which can be found in a typical urban catchment such as a neighborhood or an entire city. However, for the purposes of this project, each urban plot in the current situation and its variations under each urban development scenario is considered as an individual catchment.
Thus, the four urban fabric types identified in the Pankow neighborhood in Berlin by the urbanists of U-lab (EPFL) at the start of the WANH project are:

- Industry (A in Fig.5): is a typical industrial site with some big industrial sheds for industrial activities or the deposit of materials, a lot of open space covered in asphalt for the parking of trucks, cars and containers and smaller administrative buildings. The main characteristic which makes it unique between all the studied areas is that it is not a residential parcel. Moreover, most of the surface is sealed as it is currently covered with buildings or asphalt.
- Single family housing (B in Fig.5): Is an area which consists of single houses which often also have a garden behind them with various vegetation species (mostly grass and shrubs but even trees in some cases). The access to the front of the houses from the street is done with a path made either out of pavement or grass.
- Slabs (C in Fig.5): is a typical residential area found in the outskirts of cities. It is composed of very tall buildings slabs on the south, north and east edges of the plot. Then, right in the middle of the plot there is a park with one small building which is a school. There are also smaller housing buildings around that same central park, opposite to the big slabs as can be seen in the third photo going down in Figure 5.C. The vegetation in this area is mostly grass which covers spaces around the different buildings, along with shrubs. There are also some big trees which are found in the 'park' at the center of the plot. However, the vegetation does not seem very healthy, particularly the grass. Indeed, the places where there is supposed to be grass, mostly resemble to bare soil. Finally, there is also a wide street made of asphalt that circles around this central 'park' whose sides are used to park cars as can be seen in the second photo going down in Figure 5.C.
- Open blocks (D in Fig.5): is another typical configuration of a residential area. It is composed of four story medium size buildings which form the shape of a rectangle such as to leave a big open shared space in the middle. This shared middle space sometimes has a park and a playground for children or it has little plots of communal gardens. Either way, there are usually some big trees as well as surfaces covered in grass and shrubs covering this shared space. There are also some smaller surfaces behind the buildings which are covered in shrubs (in the side going out to the street). Interestingly, in this case, the streets around the building complexes are pavement and only the main street of the neighborhood is covered in asphalt.

Figure 5: Map with a general overview of the modelled areas inside the Panke-Pankow sub-catchment in Berlin, Germany. Satellite pictures of each studied urban parcel representing different urban fabric types: **A** corresponds to the Industry, **B** corresponds to the Single Family Housing, **C** corresponds to the Slabs and **D** corresponds to the Open Blocks. Photos taken during a visit to Berlin further illustrate each of the modelled areas.

2.4.3 Urban scenarios

Three different urban scenarios are studied in this project. The first one corresponds to the current state of each urban fabric type. The others, however, correspond to potential future alternatives achieved by different urban development strategies by making some changes in the landcover in each of the different urban fabric types. The main idea driving the research around these future scenarios is that the effects of the urban architecture on the water cycle can be reduced. Indeed, in urban areas, a large portion of rainfall runs off sealed surfaces, creating flash floods and reducing infiltration and therefore groundwater recharge Gillefalk et al., 2021. Therefore, the objective of the urbanists from Lab-U (EPFL), as a part of the WANH project, was to create two different urban development scenarios which are built by making some realistic changes in landcover such as to reduce the amount of 'impermeable' surfaces for the different urban fabric types and increase the water retention and groundwater recharge potential. The first scenario is made of landcover changes which are more conservative as the changes which are proposed are pretty straightforward to implement whilst the second scenario is made by applying the same changes as in the conservative scenario and making further changes which are more difficult to implement. The initiatives behind the changes implemented in both scenarios are explained in more detail hereafter.

Conservative scenario

Four different initiatives drive the landcover changes implemented in the conservative scenario for the different urban fabric types. The main focus being to enhance the permeability of surfaces and the effects of vegetation on the water cycle.

- The first initiative which is followed is to transform parking lots. The goal is to select surfaces devoted to car and truck parking which can be de-paved such as for example the parking spots on the side of the street inside the Slabs area shown in Figure 6a. Indeed, asphalt and pavement can be replaced with stabilized grass surfaces as can be seen in Figures 6b and 6c which show parking spaces which followed this principle in another area of the Pankow neighborhood.

(a)

(b)

(c)

Figure 6: Example of measure implemented in the conservative and radical scenarios: parking lots are not covered in asphalt or pavement anymore (as in Figure(a)) but in stabilized grass surfaces as it is already done in some other places inside the Pankow neighborhood (Figures (b) and (c)).

- The second initiative is to transform sidewalks. The sidewalks are currently mainly covered in pavement or asphalt as can be seen in Figure 7. The goal is to select sidewalks which can be transformed both in their width and their depth. The sealed surfaces can then be replaced with more permeable materials. Furthermore, in the objective of improving vegetation inside the urban areas, rows of trees can be systematically planted along sidewalks as it is already sometimes the case as can also be seen in Figure 7.

Figure 7: Example of sidewalk in the OpenBlocks parcel

- The third initiative consists in transforming public buildings' open spaces. This refers to open spaces located on the grounds of public buildings such as schools, police stations, etc.. These can be heavily transformed through the depaving of most sealed surfaces and the planting of new vegetation. This is an example of the main initiative which leads to landcover changes in the central park of the Slabs area.
- The fourth and final initiative is to regenerate lawns. Indeed, lawn surfaces, mainly the ones located in front of or in between collective housing buildings, as well as inside private gardens can be more densely vegetated. Grass can be let to grow longer, and more shrubs can be planted on underused areas. This improves the effects of vegetation on the water cycle in the urban area as the quality of vegetation surfaces is enhanced as well as the quantity.

Radical scenario

As explained before, in the radical scenario all the initiatives behind the changes in the conservative scenario are taken into account. However, three other initiatives are also implemented which lead to new changes in the landcover in the different urban fabric types. The goal of these initiatives however does not change. Indeed, the objective remains to enhance the amount of permeable surfaces.

- The first initiative consists in depaving secondary streets. Indeed, secondary streets which only receive local car traffic can be de-paved. Therefore, asphalt and pavement covering the streets (such as shown in Figure 8) are replaced with more permeable gravel surfaces which still allow for slow motorized mobility.
- The second initiative consists in vegetating flat roofs. Flat roofs are systematically transformed into «green» roofs which are capable of temporarily storing some water. It is important to note that this measure is in agreement with current politics of urbanisation in Berlin as owners can now receive a grant to evaluate the possibility to transform their normal roofs into vegetated roofs and to implement the modifications if the transformation is estimated to be worth it ("GründachPLUS – Berlin Senate promotes green roofs", 2020).
- The third initiative aims to transform residual sealed surfaces. These «residual» sealed surfaces correspond to all surfaces which are neither used for parking, walking, driving, recreation or storing purposes. Examples of such surfaces are all the immediate surfaces surrounding buildings or the edge of the street as it becomes sidewalk. These surfaces are de-paved and planted with vegetation, while allowing for multiple uses.

The initiatives hereby explained for each scenario of urban development were applied to each of the urban fabric types by the urbanists. This yielded new landcover maps which are used in this project to run the simulations of the conservative scenario and radical scenario for each urban fabric type.

(a) Paved streets in the OpenBlocks parcel

(b) Asphalt covered streets in the Slabs parcel

Figure 8: Example of original paved streets and streets covered with asphalt. Secondary streets of this type will have their surfaces replaced by more permeable gravel surfaces.

3 Results

In this part of the report, the results obtained using the methods explained in the previous section are shown. The aim is to gain insights into the partitioning of each specific chosen rainfall event and its transit time inside each urban landscape by understanding the travel time distribution of each output flux. However, first, to better understand the results, a little analysis of the landcover composition each modelled urban plot is done. Indeed, the following sections of this report mean to quantify to which extent the changes in landcover described here next affect the partitioning of rainfall water, the overall transit time of water and the travel time distribution of the different output fluxes inside the different urban fabric types for the different scenarios and seasons.

3.1 Analysis of the landcover of each modelled catchment

The first result that is obtained in this project, before even launching the simulations using the EcH$_2$O-iso model, is the proportion of the different landcover types in each urban fabric type for each urban development scenario. Figure 9 therefore shows the fraction that each landcover represents in each urban catchment which is modelled and studied in this project.
As was explained before, the general goal of the landcover changes between the different scenarios is to increase the amount of permeable areas inside each urban catchment because it is expected to reduce the amount of rainfall going into surface runoff and increase infiltration of water into the soil which then becomes available and can be used by vegetation or can leak into the deeper parts of the soil and thus become groundwater recharge.
The landcovers which are considered as permeable in this project correspond to all vegetation landcovers (grass, shrub and trees) and also incorporates gravel and vegetated roofs (which only exist in the radical scenario). Indeed, gravel is considered a very permeable surface. The rest of the landcovers (asphalt, building and pavement) are considered as sealed surfaces as they have very low permeability.

Urban fabric type	**Scenario**	**Fraction of permeable areas (%)**	**Fraction of vegetated areas (%)**
Open Blocks	Current situation	45.8	42.2
	Conservative	52.9	49.3
	Radical	72.2	60.7
Slabs	Current situation	48.2	38.4
	Conservative	55.7	48.1
	Radical	73.2	62.4
Single Family Housing	Current situation	56.8	55.3
	Conservative	62.5	60.8
	Radical	86.1	74.4
Industry	Current situation	14.3	13.0
	Conservative	25.2	23.9
	Radical	72.7	53.9

Table 1: Difference in the fraction of permeable areas and vegetated areas between the different urban fabric types and between the different urban development scenarios

Table 1 shows that when the urban plots transition from the current situation to the conservative scenario, the overall fraction of areas covered in vegetation increases. Indeed, Figure 9 shows that even though the fraction of grass covered surfaces decreases in all urban fabric types except the Industry, more shrubs are planted than the ones necessary to compensate. Furthermore, trees are planted alongside the sidewalks as often as it is possible. Therefore, the overall fraction of vegetated areas increases in each urban catchment corresponding to the objective of rehabilitating existing vegetation but also to have denser vegetation.
Furthermore, it is interesting to notice that the increase in permeable areas in all fabric types is mostly due to this increase in vegetated areas. Indeed, the increase in vegetated areas directly lead to the increase of the overall fraction of permeable areas by 7.1% in the Open Blocks, by 7.5% in the Slabs, by 5.7% in the Single Family Housing and by 10.9% in the Industry between the existing conditions and the conservative scenario.

The increase in the fraction of permeable areas between the current situation and the radical scenario for all urban fabric types is also clearly visible in Table 1. Indeed, with the changes made in the radical

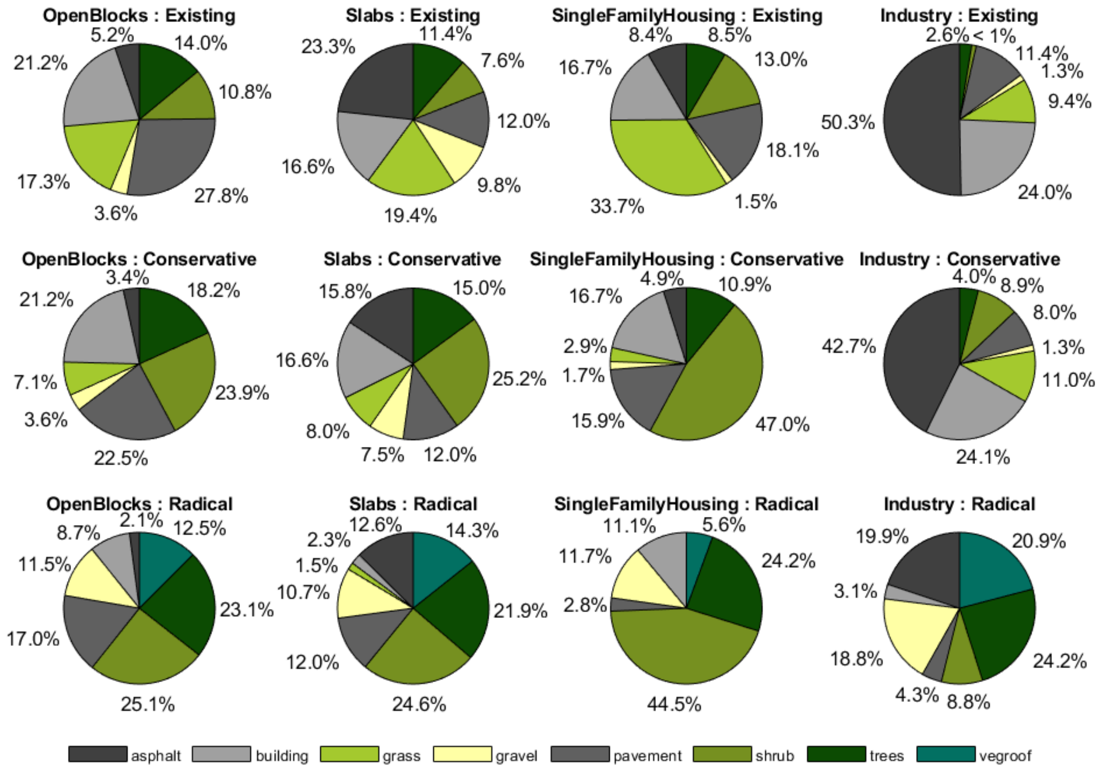

Figure 9: Fractions of landcover types in each urban fabric type and each studied scenario.

scenario, the permeable areas cover around 30% more of the total surface compared to the current situation of each urban fabric type, except for the Industry which has the most noticeable increase in the fraction of permeable areas as it is five times higher (which corresponds to an increase of 58.4% in permeable surfaces) in the radical scenario compared to the current situation.
Moreover, from Figure 9, it is noticeable that this important increase in permeable areas in the radical scenario is mostly due to a transition from asphalt and pavement to gravel surfaces in streets and sidewalks and to the installation of vegetated roofs on most buildings in each urban fabric on top of the addition of more trees and shrubs than in the conservative scenario.

3.2 Ecohydrological partitioning of rainfall

A lot of information can be gained from analysing the cumulated normalized breakthrough curves of each output flux. Indeed, one can extract the partitioning of rainfall by reading the proportion of cumulated tracer mass present in each flux with respect to the total amount of tracer mass input into the catchment at a given point in time.

Figure 10 represents the cumulated NMBTC of the ET flux, the sum of the NMBTCs of the ET flux and surface runoff together and finally the sum of the NMBTCs of all output fluxes together in the OpenBlocks for each studied scenario and both seasons of rainfall tracked. It thus shows the partitioning of water from winter rainfall (in the left plot) and summer rainfall (in the right plot).
However, given that the analysis period following each rainfall event doesn't have the same duration for the summer and winter rainfall events, it is decided to analyse the partitioning of rainwater for each season one year after the respective start of the tracer input (i.e. the start of the tracked rainfall) to be able to do comparisons. Indeed, it is possible to interpret the value reached by each NMBTC at the 365 day mark as the proportion of rainwater that exits the urban catchment through the ET flux, the ET flux and surface runoff combined and all output fluxes combined which therefore corresponds to the total amount of rainfall having left the catchment one year after the start of the tracked rain event. The differences between the curves therefore give the proportion of rainfall having left the catchment through each output flux.
As such, the plot on the left of Figure 10, shows that 1 year after the start of the winter rain, most of the

water, 57% went into surface runoff and only 11.6% of rainwater went into evapotranspiration and 8.1% into groundwater recharge in the current scenario. The plot on the right in turn shows that in summer rainwater gets partitioned very differently than in winter as 50.5% went into evapotranspiration and only 27% went into surface runoff and 5.5% into groundwater recharge 1 year after the start of the summer rainfall in the current scenario.
This can be explained by the fact that in summer a lot more evapotranspiration occurs compared to winter. Indeed, as it gets hotter, plants transpire more and pump more rainwater stored in the soil thus reducing the fraction of rainfall available for groundwater recharge.
Furthermore, hotter temperatures lead to an increase of the evaporation rate and infiltration rate which explains the significant decrease in the amount of rainwater exiting the catchment as surface runoff in summer compared to winter and increase in evapotranspiration. Indeed, more water will infiltrate into the soil as it was a very dry summer in 2018 in Germany and a soil with low water content has more infiltration capacity ("KIT - Drought Affected about 90% of the German Territory", 2021; Diamond and Shanley, 2003).
Moreover, the water which does not infiltrate the soil will have a higher tendency to evaporate because of the hotter temperatures as it ponds into the surface before becoming runoff.
Finally, there is also a decrease in rainwater which becomes groundwater recharge in summer compared to winter. This is mostly explained by the increase in evapotranspiration as was mentioned before. Indeed, even if in summer more water infiltrates into the soil compared to winter, since the plants transpire a lot more water in hotter conditions, a very important fraction of the stored water is redirected into evapotranspiration in summer and is therefore not able to reach the groundwater.

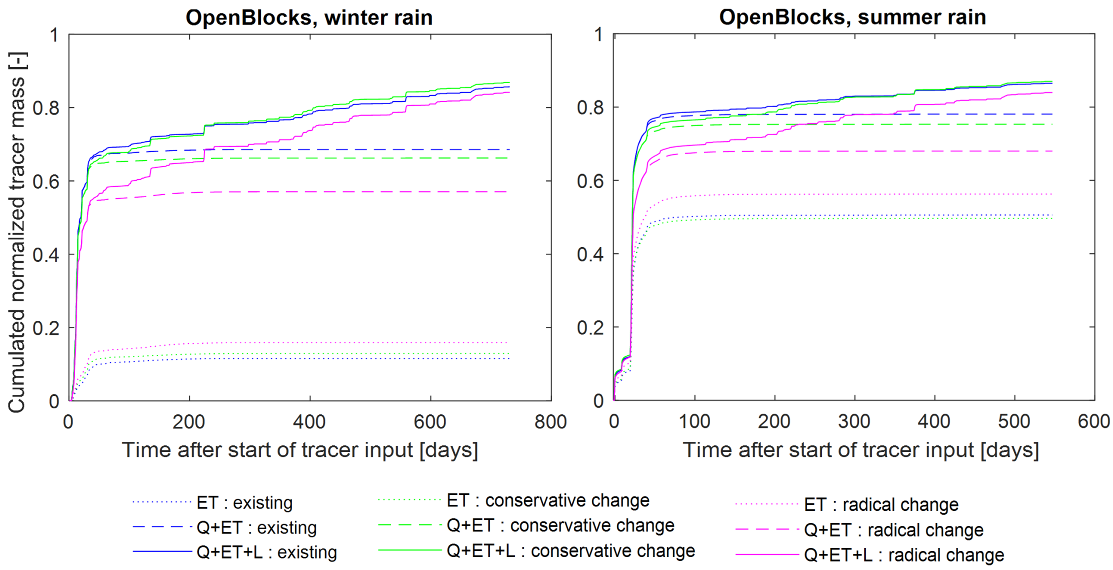

Figure 10: Cumulative NMBTCs of the output fluxes summed together for the Open Blocks catchment in the current situation. On the left are the results for the winter rain tracked and on the right are the results for the summer rain. The dotted line represents the cumulative NMBTC of evapotranspiration, the dashed line represents the cumulative NMBTCs of evapotranspiration and surface runoff summed together and the full line represents the cumulative NMBTCs of evapotranspiration, surface runoff and leakage summed together. The results for the current situation are shown in blue, the ones for the conservative scenario in green and the radical scenario in pink.

Figure 10 also shows another interesting fact when looking at the end of all simulations (being it winter or summer rain and either scenario): the total mass of tracer input into the catchment isn't recovered by the analysed output fluxes.
Indeed, the plots show that in no simulation does the sum of the cumulated NMBTCs of evapotranspiration (ET), leakage and surface runoff reach 1 at the end of the simulations. However, the NMBTCs corresponding to ET alone and ET and surface runoff summed together reach a constant value in both seasons after approximately 200 days. This means that ET and surface runoff already took up all the possible rainwater after 200 days.
Moreover, the curve corresponding to all three output fluxes added together is still increasing by the end

of the simulation which means that the maximum amount of rainfall retrieved as leakage is not reached by the end of the simulation.
Therefore, we can assume that the missing tracer mass not yet recovered by the end of the simulations corresponds to water which will be leaving as leakage eventually. This is why, for the computation of the TTD curve of leakage explored in the next section, the fraction of rainfall partitioning into leakage is computed as the sum of the observed fraction of rainfall that goes into leakage by the end of a simulation and the fraction of rainfall which is still not recovered by any output flux by the end of said simulation.

The previous analysis only focused on the current situation of the OpenBlocks parcel for both seasons. However, from Figure 11, it is possible to say that the partitioning of rainfall follows the same trend in each season in all urban fabric types for the current situation. Indeed, in all cases, the fraction of rainwater exiting each catchment as surface runoff exceeds 50% in winter and the fraction of rainwater that reaches the groundwater is higher in winter than in summer. Moreover, in all cases more rainwater exits the catchment as evapotranspiration in summer; but it is important to notice it does not always exceed the amount going into surface runoff. Indeed, if there are not enough vegetated surfaces in an urban catchment, as for example in the Industry, rainfall still mostly leaves the system through runoff in both seasons.

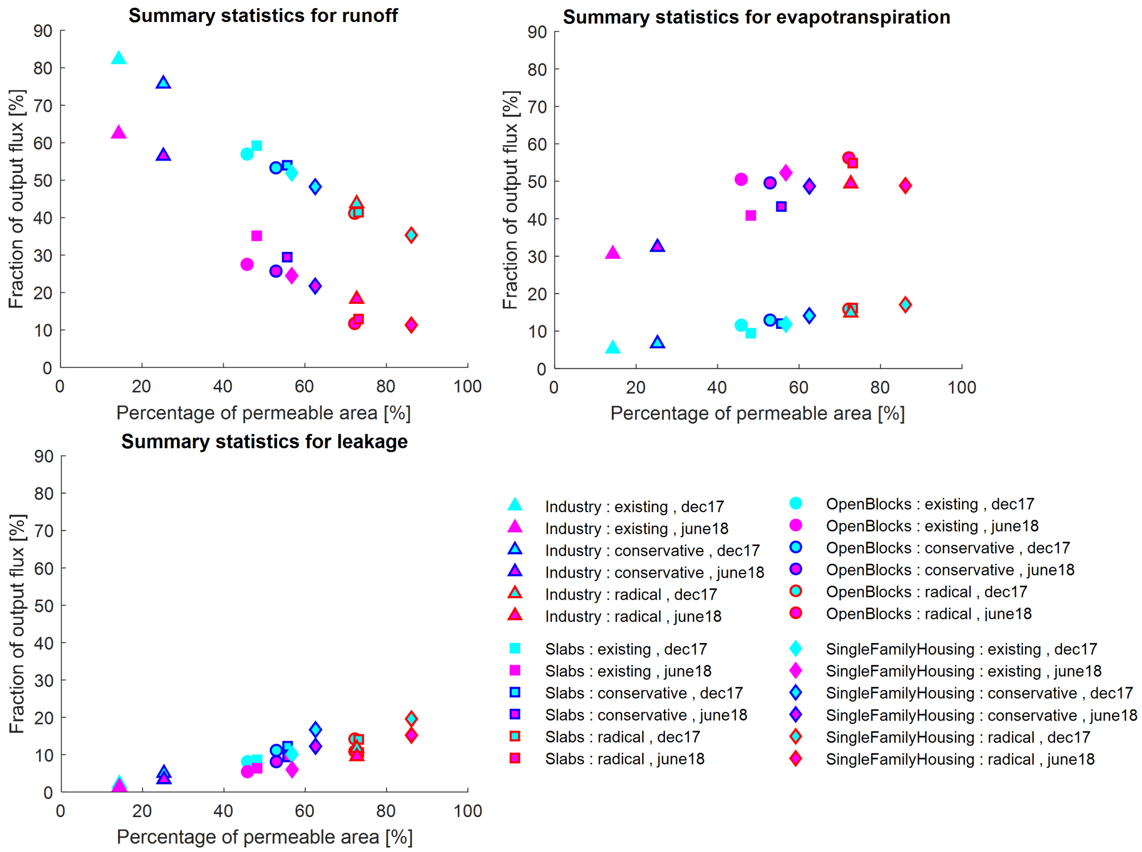

Figure 11: Summary statistics showing the partitioning of rainfall into each output flux depending on the proportion of permeable areas in each catchment studied. This plots were found by combining the results of the changes in landcover in each urban fabric type for each scenario and the partitioning of rainwater between the different output fluxes one year after the input of the tracer into each catchment.

Figure 10 also allows to compare how the partitioning of rainwater is affected by changes in landcover in the OpenBlocks.
Indeed, on the one hand, leakage increases by 3% in summer and 2.5% in winter in the conservative scenario and by 5% in summer and 6% in winter in the radical scenario compared to the current situation. Evapotranspiration, on the other hand, actually decreases by 1% in summer and increases by 2.5% in winter in the conservative scenario and increases by 6% in summer and 4% in winter in the radical scenario.
Moreover, it is interesting to notice that even if the original proportion of rainfall flowing into surface runoff is very different in each season in each scenario, the amount by which the fraction of rainfall going

into surface runoff is reduced is very similar in both cases. In fact, the fraction of rainfall exiting the catchment as surface runoff is reduced by around 2.5% when conservative landcover changes are applied and by around 13% when radical landcover changes are applied to the OpenBlocks, in both seasons.
Therefore, as the changes in partitioning are more important in the radical scenario than the conservative scenario compared to the current situation, it is possible to say there is a decrease in the amount of rainfall becoming surface runoff when more permeable surfaces are integrated in the OpenBlocks while there is an increase in the amount of water leaving in the form of evapotranspiration and groundwater recharge.

The previous analysis finds the main trends for the partitioning of rainfall between the different scenarios for the OpenBlocks but Figure 11 shows that the same trends also apply to the other urban fabric types studied. Indeed, it is clear that the fraction of rainfall exiting a certain urban plot through surface runoff decreases as the total amount of permeable areas increases inside said urban plot while the fraction of rainwater going into evapotranspiration and leakage increases as the fraction of permeable areas increases, independently of the season.
However, it must be noticed that the amount of change in rainfall partitioning depends a lot on the urban fabric type and most importantly on the adopted scenario. In the Industry for example, the changes in landcover adopted in the conservative scenario are not enough to change the overall partitioning of rainfall. Indeed, more than 50% of rainfall still exits the catchment trough surface runoff both in winter and in summer in the conservative scenario. The big change in the partitioning of rainfall only occurs when radical changes are applied and the amount of permeable areas becomes five times more important than in current situation. Indeed, in the radical scenario, 43.8% of rainfall runs off the catchment in winter and 18.3% in summer thus allowing for a significant increase in the amount of water that infiltrates the soil and becomes available for plants or flows into the groundwater.

3.3 Travel time distribution curves of the output fluxes

This part of the results focuses in analysing the travel time distribution curve of each of the output fluxes: evapotranspiration, surface runoff and groundwater recharge. Travel time distribution curves allow to estimate the transit time of the rainwater parcels which leave a catchment through a certain output flux. Furthermore, they allow to compare the 'velocity' of the rainwater parcels which leave a catchment through a certain output flux from one scenario or season to another because even if the quantity of water leaving the catchment through a certain flux increases, the transit time of water should remain the same as the distance travelled by the water parcel does not change.

The detailed analysis on the differences in transit time of water leaving the catchment through each output flux focuses again only on the OpenBlocks urban fabric type.

Figure 12 shows that each output flux has a very different timescale for taking rainwater out of the system and that this timescale is very similar for surface runoff and leakage fluxes between the seasons but that it seems to diverge a little between the seasons for evapotranspiration.
As expected, rainwater leaves the catchment through surface runoff almost immediately in both seasons and in all scenarios, it has a very short transit time. Indeed, the TTD curves show that in winter, 32 days after the start of the tracer input (which corresponds to the 31st of December), a 100% of the mass going into surface runoff is reached and in summer, the 100% is reached after 23 days since it stops raining the 24th of June. Therefore, the day the last raindrop falls into the catchment, is the day that all water partitioned into surface runoff leaves catchment. Moreover, this trend seems to be the same for all scenarios.
In contrast, the leakage or groundwater recharge does not start until 1 month after the start of the summer rainfall event and 40 days after the start of the winter rainfall event. Moreover, only 25% of the rainwater which is partitioned as groundwater recharge left the catchment after one year in both seasons in the current scenario. This means that rainwater partitioned into leakage flows very slowly out of the catchment, it has a long transit time. However, when changes in the landcover occur and the proportion of permeable areas increases inside the catchment, 33% of the rainwater which is partitioned as groundwater recharge left the catchment after 1 year in winter and 34% in summer for both new urban development scenarios (conservative and radical scenarios). Therefore, water partitioning into leakage seems to leave the catchment at the a very similar speed each season but faster if there are more permeable areas inside the catchment. It is important to note that the TTD curve of leakage does not reach 1 by the end of a simulation because, as mentioned before, the total amount of rainfall leaving the catchment through

leakage is considered to be the sum of the fraction of rainfall that actually went into leakage by the end of a simulation and the fraction of rainfall that still has not exited the catchment by the end of said simulation.

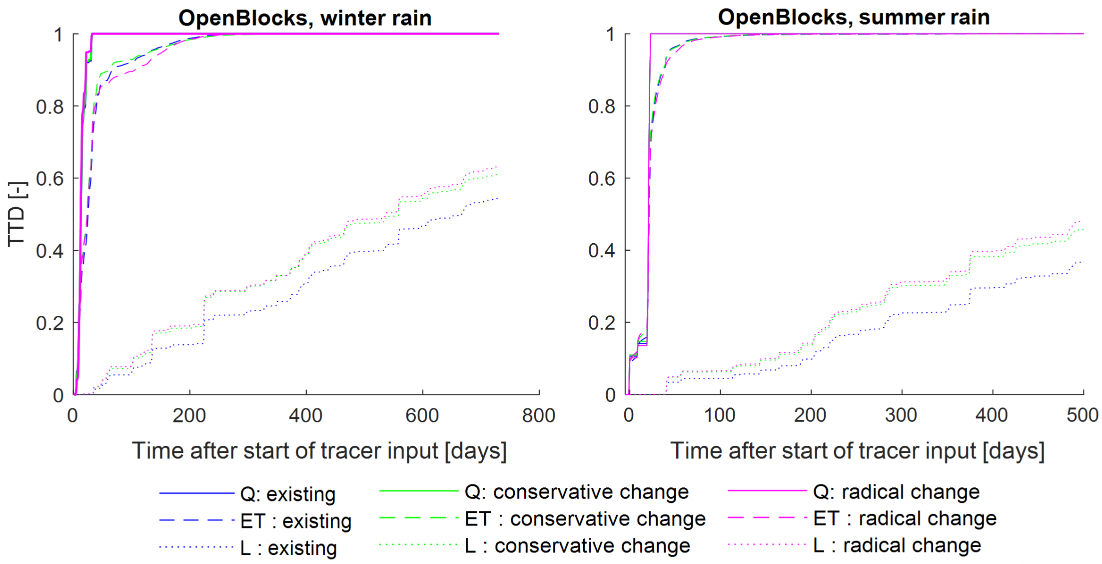

Figure 12: The plot on the left shows the TTD curves of all the output fluxes (Q : surface runoff, ET: evapotranspiration, L: leakage) for the winter rainfall for the OpenBlocks and all urban scenarios. The plot on the right shows the TTD curves of all the output fluxes for the summer rainfall for the OpenBlocks and all urban scenarios.

Finally, water parcels leaving the catchment through evapotranspiration have a rather short transit time which is dependent on the season of the rainfall event. As can be seen, in both cases, evapotranspiration starts using rainwater immediately at the beginning of the rainfall event and makes most of the rainfall partitioned into evapotranspiration leave the catchment by the end of the rain event. However, there is an important difference for the time it takes for evapotranspiration to use up all the rainwater between the seasons. Indeed, at the end of the winter rain, 75% of the rainwater partitioned as evapotranspiration already left the catchment while for the summer rain it amounts to 70%. Moreover, it takes around 7 months to completely use winter rainfall water while it only takes 4.5 months to completely use summer rainfall water independently of the scenario. Thus, it seems that water is flowing faster out of the catchment through evapotranspiration in summer compared to winter for every scenario. Furthermore, the left plot shows that water partitioned into evapotranspiration seems to leave the catchment slower in the first months that follow the winter rain event in the new urban development scenarios, especially in the radical scenario. Therefore, water partitioning into evapotranspiration seems to leave the catchment faster in summer than in winter and faster in the first months that follow the rain event when there are more sealed surfaces inside the catchment.

These trends regarding the general travel times of each output flux presented for the OpenBlocks are the same for the other urban fabric types (the TTD plots for all other simulations are shown in Figures A3, A4 and A5). Indeed, in all cases, the surface runoff takes rainwater immediately out of the system in both seasons. Moreover, leakage does not start after approximately 1 month after the start of each rain event and takes less than half of the rainwater partitioned into groundwater recharge out of the system after one year. Finally, evapotranspiration takes most rainwater out of the system by the end of each rain event and the rest of it faster in summer than in winter. However, one noticeable difference for the travel time distribution of the evapotranspiration flux is that in the Industry, most rainwater partitioned as evapotranspiration does not leave the catchment immediately as only half left 1 month after the start of the winter rainfall event while for the other urban fabric types 60% or more rainwater has left the catchment through evapotranspiration 1 month after the start of the winter rain. This is most probably due to the fact that there is not much vegetation using rainwater to transpire immediately after the start of the rainfall events in the Industry.

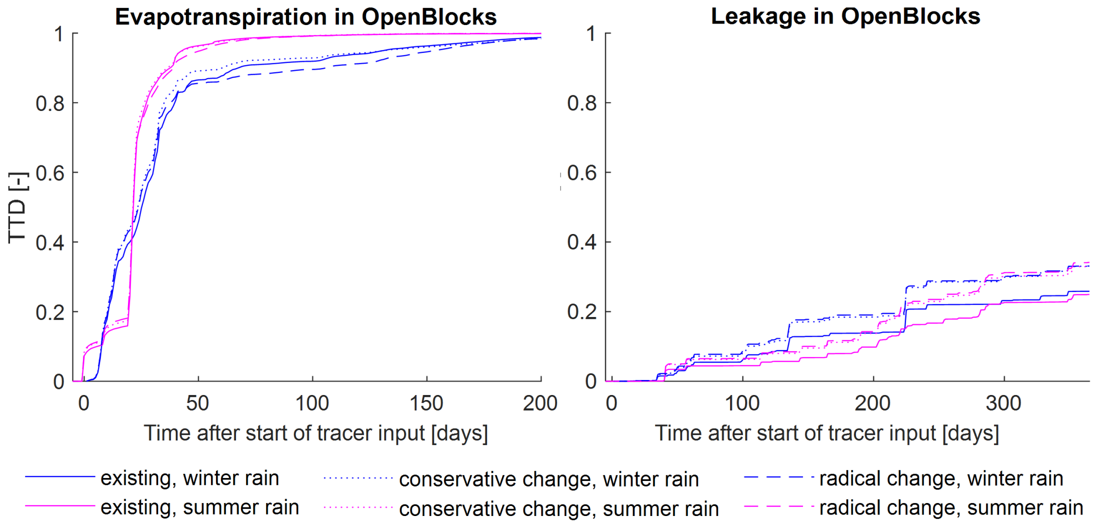

Figure 13: The plot on the left shows the TTD curves of the evapotranspiration flux for the OpenBlocks and all urban scenarios for the winter and summer rainfall events. The plot on the right shows the TTD curves of the leakage flux for the OpenBlocks and all urban scenarios for the winter and summer rainfall events.

Figure 13 allows to get more detailed insights into the difference in travel time dynamics grossly observed before for the evapotranspiration flux and the leakage flux between summer and winter rainfall in the OpenBlocks for all scenarios through the comparison of the respective TTD curves.
Thus, the left plot shows that a 100 days after the tracer input (beginning of the tracked rainfall events), in summer, all the rainwater partitioned into evapotranspiration has left while in winter only 90%. Therefore, water parcels being drawn out of the system by evapotranspiration are indeed moving faster in summer than in winter and most probably due to the fact that in summer, the hotter temperatures increase the evapotranspiration rate, thus making water move faster through the plants.
Moreover, the same plot clearly shows the differences in the travel time distribution of rainfall going into evapotranspiration between the different scenarios in the OpenBlocks. Indeed, for the winter rainfall, only 89% of the water partitioned into evapotranspiration has gone out of the system 90 days after the start of the rainfall in the radical scenario while the fraction amounts to 91% in the current situation. However, interestingly, more winter rainfall left the catchment through evapotranspiration in the conservative scenario compared to the current situation after 90 days. Indeed, in the conservative scenario 92.6% of the rainfall partitioned into evapotranspiration has left the catchment 90 days after the start of the winter rainfall event. This difference is most probably due to a change in the proportion of vegetation species found inside the catchment for each scenario and the fact that they all have a different partitioning in the fluxes composing the evapotranspiration flux (soil evaporation, transpiration and evaporation of intercepted rainfall) and that each of these fluxes has a different travel time distribution for water too. Furthermore, it is clear that for the summer rainfall, the water parcels all move out of the system at the a very similar velocity independently of the scenario. This is most probably due to the fact that the main driver of the increase in the rate of evapotranspiration is the hot temperatures which are the same in every scenario. Therefore, winter rainfall partitioned into evapotranspiration can move slower or faster inside an urban catchment depending on the proportion of each type of vegetation found inside the catchment while in summer all the water always moves at the same speed.
Finally, another interesting detail can be seen on the same plot concerns the moment at which after the start of the rain event vegetation starts using rainwater which infiltrated the soil. Indeed, the plot shows that in summer, vegetation starts using the water right away whilst it takes a around week in winter. This most probably comes from the fact that in summer, as mentioned previously, there was a drought in Berlin which means that the plants were in need of water but had a dry soil. Thus, as the water storage build up and water became available right when it started to rain, the different vegetation species tapped into it right away. However, in winter, the soil most probably already had sufficient moisture to cover some of the water needs of the vegetation the days it started to rain thus adding some delay to the moment vegetation started to use the newly infiltrated rainwater.

The right plot in Figure 13 instead shows the comparison of the TTD curves for rainfall partitioned into leakage between summer and winter rainfall in the OpenBlocks and for the different scenarios. It is interesting to notice that water seems to be exiting the catchment through leakage faster in winter than in summer at some specific moments even if after 1 year almost the same amount of water has left the catchment. This small difference in the end is most probably due to higher soil moisture in winter and thus a higher conductivity than in summer which makes water flow a little faster. However, there are much bigger differences in the months following the rain event such as 150 days after the start of each rainfall event where only 6.7% of water partitioned into leakage left the catchment in summer while in winter 12.8%, almost double or a similar phenomenon observed 250 days after the start of the rainfall events. These moments where water is leaving much faster through leakage in winter than in summer correspond to short and very intense rainfall events that occurred in the months following the winter rain event (see Figure 1). Thus, as more water is infiltrating the soil it "pushes" the older water parcels down which in this case correspond to the water parcels from the tracked winter rainfall event. Indeed, in summer, there is only one such intense rainfall event which marks the first major release of rainwater into the groundwater on the 11th of July 2018 or 40 days after the start of the tracked summer rainfall event. However, in the summer months that follow after there are no other important rainfall events which explains the constant release of little amounts of rainwater into the groundwater as seen on the plot.

Furthermore, the plot shows that in the conservative and radical scenarios, water is flowing faster through the soil column than in the current situation. Indeed, the travel time distribution curves always show higher amounts of rainwater being leaked into groundwater for the new urban development scenarios compared to the current situation. This can again be explained by the fact that rainfall is infiltrating a soil which is more saturated because the new scenarios increase the amount of permeable areas in the catchment so more rainwater is infiltrating the soil both before and after the tracked rain events thus making the soil more saturated which makes the hydraulic conductivity increase and makes water flow faster and leads to having more water parcels which can 'push down' the older water from the track rain events. Meanwhile, in the current situation, the tracked rainfall is infiltrating into a dryer soil because there is less infiltration overall because of less permeable surfaces inside the catchment. Therefore, the rainwater moves slower through the soil column in the current situation compared to the conservative and radical scenarios and leaves the catchment through leakage at a later time.

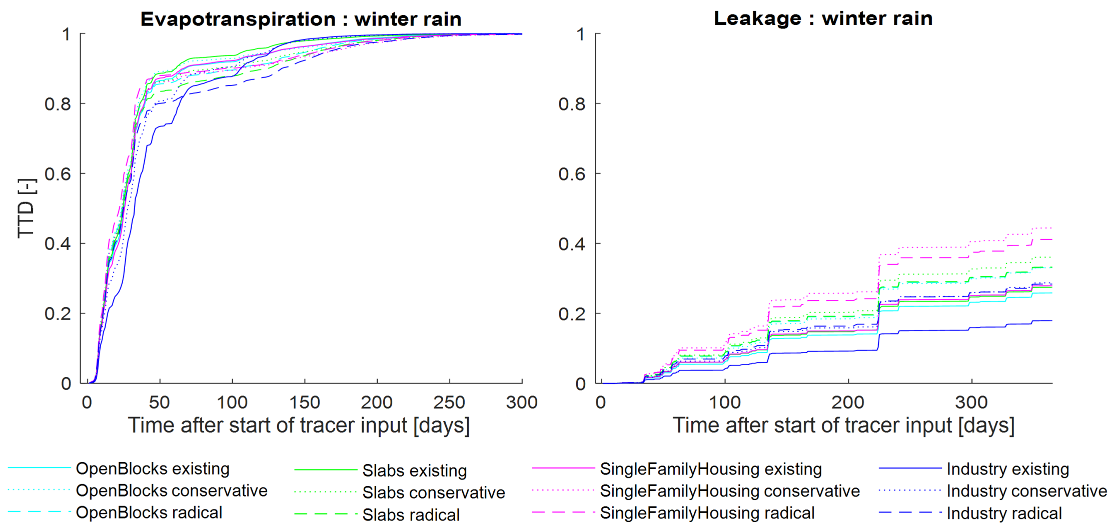

Figure 14: The plot on the left shows the TTD curves of the evapotranspiration flux for all urban fabric types and scenarios for the winter rainfall event. The plot on the right shows the TTD curves of the leakage flux for all urban fabric types and scenarios for the winter rainfall event.

The previous analysis of the evapotranspiration and leakage fluxes only focused on the OpenBlocks. Therefore, to have a global comparison between all the simulations, Figure 14 shows the difference of the TTD curves of the evapotranspiration flux and the leakage flux between the different urban fabric types and the different scenarios for the winter rainfall.

On the one hand, on the left plot, it can be seen that the evapotranspiration flux has a unique TTD curve in each urban fabric type and for each scenario. The differences between the curves of each urban fabric type for each scenario can be explained by the fact that each catchment has a unique distribution

in landcover types as Figure 9 had shown.
Moreover, each catchment has a particular species composition for the vegetated areas and this leads to variations in the TTD of the evapotranspiration flux. Indeed, each species has a particular partitioning of the evapotranspiration flux in itself since it is composed of soil evaporation, intercepted rainwater evaporation and transpiration.
Therefore, for example, for urban fabric types which have a lot more permeable surfaces, the water has a tendency to leave slower through the evapotranspiration flux as the vegetated areas tend to reduce the amount soil evaporation which is the fastest process within the evapotranspiration flux. Indeed, the TTD curves for the conservative and radical scenarios of the Slabs and SingleFamilyHousing show lower values than the TTD curves for the current situation in the first months that follow the winter rainfall event (before they all converge 250 days after the start of the rainfall event, when all the water possible left through the evapotranspiration flux). Moreover, the increase in trees which take more time to take up water for the transpiration flux while reducing the soil evaporation flux also allows to slow the velocity of the evapotranspiration flux down in the radical scenario compared to the other scenarios for these urban fabric types.
However, there is an outlier in the plot. Indeed, the Industry shows a different dynamic for the evapotranspiration flux for the current situation and the conservative scenario. This has to do with the fact that there is very little vegetation in these catchments. Therefore, it can not be easily compared with the other urban fabric types for these scenarios. However, it is interesting to see that in the radical scenario, when the vegetated areas cover more than half of the surface and the overall amount of permeable areas resembles the one of the other fabric types, the same behavior explained before can be observed. Indeed, as the amount of vegetated areas and permeable areas increases drastically in the Industry in the radical scenario, the TTD curve follows the same dynamic than the TTD curves of the other urban fabric types, especially the one of the Slabs in the radical scenario.

On the other hand, the right plot of Figure 14 shows that the TTD curves for leakage are not identical between the different urban fabric types and scenarios and don't follow any clear trend either. Indeed, there is no clear relationship between the increase in permeable areas and the velocity of rainfall parcels partitioned into leakage. However, the differences observed between all urban fabric types and scenarios can also be explained by the unique combination of landcover types making up the fraction of permeable areas inside each catchment. Indeed, the combination of landcovers with different permeabilities changes for each urban fabric type and scenario and not in a linear way compared to the amount of rainfall partitioning into leakage leading thus to different travel time distribution curves. As an example of a complex effect of a certain landcover on the travel time of leakage, the transformation of traditional roofs into vegetated roofs can be cited. Indeed, the rainwater in this case flows into the soil of the vegetated roof but the part which is not used up for evapotranspiration can not leak directly into the groundwater. Instead, the water that isn't used up for evapotranspiration ponds onto the vegetated soil and then runoffs onto the ground next to the building where it can infiltrate the "real" soil and finally trickle through the whole soil column to reach the groundwater.

3.4 Transit time of rainfall

The overall transit time of rainfall inside each urban landscape can be estimated from the sum of the cumulative NMBTCs of all output fluxes. Indeed, such a curve can be interpreted as the total amount of rainfall having left the catchment at a certain point in time. Therefore, if more rainwater has left a catchment at a certain point in time compared to another catchment, the rainfall in the first catchment can be said to have a lower transit time as it takes less time for it to leave.

Figure 15 allows to compare the overall time it takes for winter rainfall and for summer rainfall to flow out of the catchment.
It can be seen in the figure that winter rainfall resides more time inside the OpenBlocks catchment than summer rainfall and in all scenarios. Indeed, there is more water having exited the catchment one year after of the winter rainfall compared to one year after the summer rainfall. In the current scenario, there is 6.9% less rainwater having exited the catchment in winter than in summer, in the conservative scenario the difference is of 6.1% and in the radical scenario it is of 7.6%.
This is given by the fact that even if there is more water infiltrating the soil in summer than in winter, there is less water which is stored a long time inside it as most of the rainwater infiltrating the soil leaves

as evapotranspiration in summer and quite rapidly as was shown in the previous sections. Moreover, the leakage flux is less important in summer than in winter and leakage is the flux which takes by far the longest to drive water out of the system as was shown in the previous section.
Therefore, the major reason that winter rainfall resides longer than summer rainfall in this urban catchment is that there is a much bigger proportion of water exiting the system through evapotranspiration in summer and that there is less exiting it through the leakage flux than in winter.

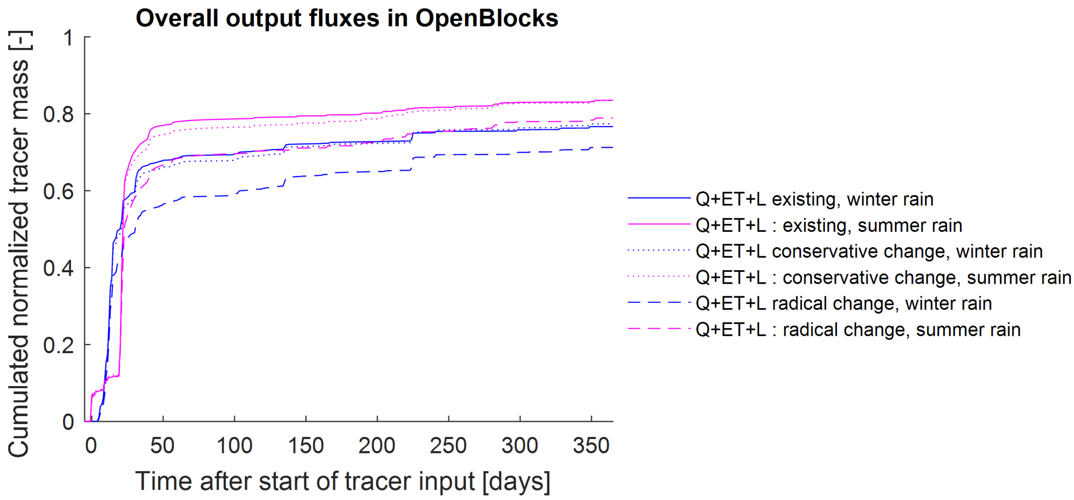

Figure 15: Cumulative NMBTCs for all output fluxes summed together for the OpenBlocks for both seasons and all scenarios studied. Each final cumulative NMBTC is obtained by summing the cumulative NMBTCs of all output fluxes in each simulation of the OpenBlocks.

It is important to notice that even if only the results for the OpenBlocks parcel are analysed here, the trend that winter rainfall has a longer residence time than summer rainfall was also noticed in all the other urban fabric types for the different scenarios as can be seen in Figure 16.
Figure 15 also shows a clear trend of the overall transit time of rainfall decreasing between the current situation and the radical scenario and this independently of the season. Indeed, one year after the start of each rainfall event studied, there is 4.5% less rainwater having left the catchment in the radical scenario than the current situation in summer and 5.4% in winter. This is can be explained by the fact that the amount of rainfall exiting the catchment through runoff decreases significantly as the proportion of permeable areas increase and that a significant fraction of this newly infiltrated water is redirected to leakage instead of evapotranspiration. Indeed, as the travel time of water for leakage is much longer than the other fluxes, if the amount of redirected water into leakage is significant enough, it can increase the overall transit time of rainfall inside the catchment. Therefore, even if in summer most of the newly infiltrated rainfall is redirected to exit the catchment through evapotranspiration, the fraction of leakage is increased enough to compensate with its slow travel time for the faster travel time of the evapotranspiration flux.
Moreover, the transit time of rainfall also decreases between the current situation and the conservative scenario but in a less significant way. Indeed, the rainfall only slows slightly down in the first 5 months following the end of the tracked rainfall event as after one year, the same amount of rainfall left the catchment in the conservative scenario and in the current situation for both seasons. As can be seen on the plot, once each of the tracked rainfall events end (meaning 1 month after the start of the tracer input), there is 2% less of rainfall leaving the catchment during 5 months. This can be due to the little decrease in the fraction of rainfall going into surface runoff. However, the overall transit time of water when looking one year after the rain events does not change most probably because the increase in the fraction of rainfall going into leakage isn't important enough to have a significant impact on the overall transit time of rainfall in the catchment.
Therefore, Figure 16 shows that for all urban fabric types there seems to be a general trend between a decrease in the proportion of rainwater leaving the system after one year and the proportion of permeable areas only for significant increases in the the amount of permeable areas. Indeed, the trend is only really respected when looking at the transition from the current situation to the radical scenario for each urban fabric type.

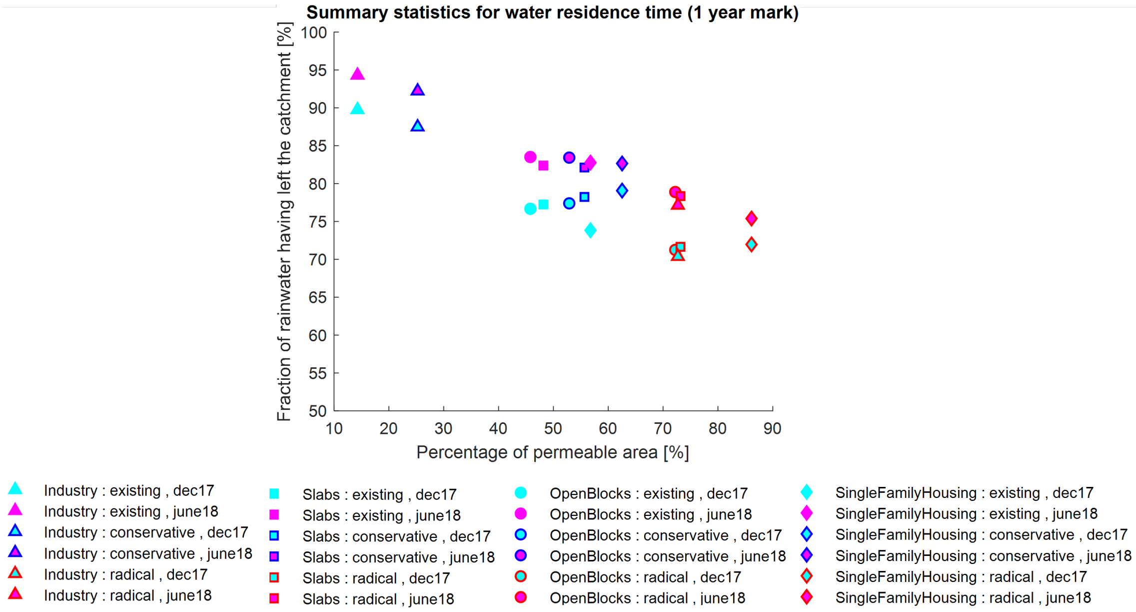

Figure 16: Fraction of rainfall having left the catchment one year after the start of the tracked rainfall events as a function of the percentage of permeable areas in each catchment. The fraction of rainfall having left the catchment is given by the total cumulated amount of tracer mass recovered after one year by all output fluxes summed together.

Figure 17 allows to compare the overall transit time of winter rainfall inside each urban fabric type and each scenario. The plot clearly shows that water in the Industry has an overall shorter transit time than all other urban fabric types as one year after the start of the rainfall event, already almost 90% of the water has left the catchment while only around 77% has left the Slabs and OpenBlocks and 75% the SingleFamilyHousing parcels in the current scenario. Indeed, all the other fabric types have very similar transit time distributions for winter rainfall.
Moreover, the same divergence between the transit time of water inside the Industry parcel and the other urban fabric types can be observed for the conservative scenario.
This divergence comes from the fact that the amount of sealed surfaces is much more important in the Industry than in all the other urban fabric types in the current situation and in the conservative scenario (as shown in Figure 9) thus leading to much more water exiting the catchment as runoff rapidly as was shown by the previous results.
However, in the radical scenario, as the Industry has a very similar proportion of permeable areas to the other urban fabric types and the amount of water going into surface runoff decreases considerably, the overall water transit time of winter rainfall becomes very similar to the one of the other fabric types.

The plot in Figure 17 also shows that with the changes in landcover in the different scenarios, the cumulated NMBTCs start to have different behaviors during the first months following the rainfall event. Even if they tend to the same point after 1 year, meaning that a very similar amount of rainfall has exited each catchment one year after the start of the rainfall event as was already mentioned before.
Indeed, on a short timescale, right after the rainfall event, it is clear that in the conservative scenario and the radical scenario less water has exited the catchment compared to the current situation. This is due to the fact that during the month of rainfall, the rainfall that leaves the catchment immediately is doing it as surface runoff and in first days that follow it is mostly related to soil evapotranspiration. However, as was seen before these fluxes are more important when there are more sealed surfaces in the catchment. Therefore, as there are more permeable areas in the conservative and radical scenarios, the amount of rainwater having left the catchment in the first month following the start of the rain event decreases.
However, there seems to be no clear trend relating an increase in the fraction of permeable areas in each urban fabric type to an increase of the overall water transit times inside the urban plots in the long term. Indeed, Figure 17 shows that at the end of the simulations, in some urban fabric types in the conservative scenario, the amount of water having left the catchment is higher than in the current situation (SingleFamilyHousing, Slabs).
This is given by the fact that, at a the medium timescale, during the months that follow the rain event, the amount of rainwater exiting the catchment is mostly dictated by the evapotranspiration flux. Moreover,

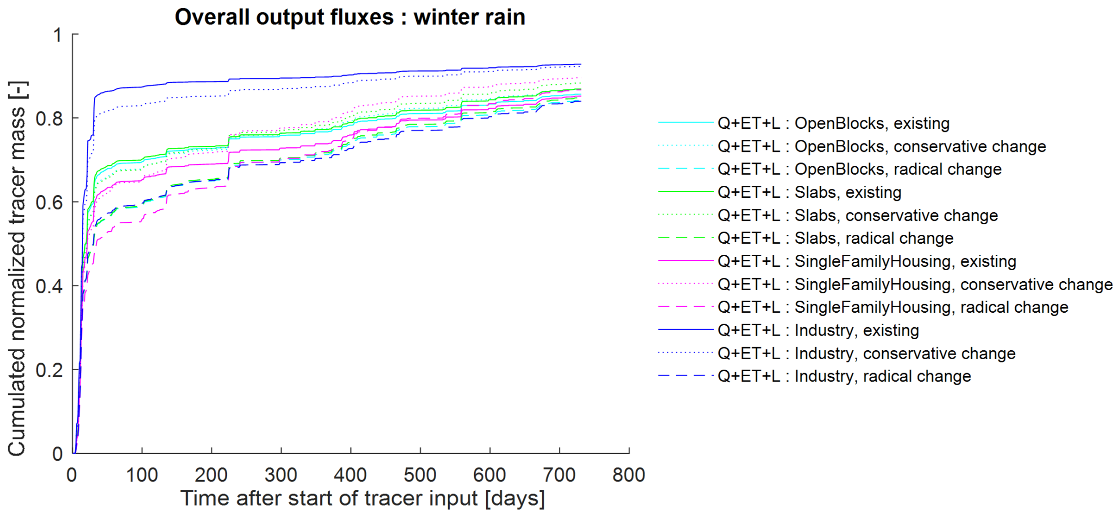

Figure 17: Sum of the cumulative NMBTCs of all output fluxes together for each urban fabric type and respective scenario for the winter rainfall.

as the particularity of the landcover changes in the conservative scenario is that the the amount of permeable areas increases mostly because of the creation of new vegetated areas, the amount of water going into evapotranspiration increases. This leads then to an increase in the rate of water being put out of the system in the 6 months that follow the rainfall event thus making the overall amount of rainwater leaving the system increase after a year compared to the current situation. It is important to recall that the leakage flux also increases with an increase in vegetated areas, and therefore permeable areas, but not sufficiently compared to evapotranspiration to have a significant impact on the overall transit time of rainfall inside the catchment.

Nonetheless, Figure 17 shows that in the case of the radical scenario, there is a decrease in the transit time of rainfall even on a long timescale for all urban fabric types except the SingleFamilyHousing compared to the current situation. The fact that the overall transit time of water inside each catchment is extended comes from an increase in the percentage of permeable areas which isn't caused by the an increase in vegetated areas solely. Indeed, in the radical scenario, secondary roads are depaved and covered with gravel instead. Gravel has a very high permeability thus allowing more water to infiltrate into the soil. However, there is no vegetation growing on these gravel patches which makes them areas where water can infiltrate the soil and reach the groundwater water easier. Thus, the increase in permeable surfaces with no vegetation allows for an increase in the amount of rainwater going into leakage. Since it takes a long time for the water to travel through the soil and reach the groundwater (as shown with the TTD curves of leakage), this increase in water partitioned into leakage allows to increase the longterm the transit time of rainfall inside the catchment.

The SingleFamilyHousing does not show the same increase in the transit time at the end of the simulation in the radical scenario compared to the existing situation because the landcover changes introduce much more vegetation than in the other urban scenarios. Indeed, there is significant increase in the amount of trees planted which leads to almost 75% of vegetation covered areas inside the catchment which in turn increases the evapotranspiration flux more than in the other urban fabric types thus leading to a higher rate of water for leaving the system in the 6 months following the rain event.

4 Discussion

4.1 What is the difference in ecohydrological partitioning and transit time of water for rainfall events in summer and winter in different urban settings?

The results show that partitioning of rainwater inside each urban catchment is highly affected by the season of the rainfall event. Indeed, in winter, there is lot more rainwater which exits the urban catchment as surface runoff than in summer. Moreover, there is a significant higher amount of rain recharging the groundwater in winter compared to summer. However, the evapotranspiration flux shows the inverse behavior as there is more rainwater leaving the catchment through evapotranspiration in summer than in winter. These trends all can be explained by the fact that in summer there are hotter temperatures than in winter. Indeed, the hotter temperatures increase the infiltration capacity of the soil, the evaporation rate of water ponding at the surface and the transpiration rate of vegetation species. Therefore, the portion of rainfall partitioning into surface runoff decreases significantly in summer compared to winter while the fraction going into evapotranspiration increases.
Moreover, the hotter temperatures in summer also increase the transpiration rate for all the different vegetation species found in the urban catchments studied. Therefore, there is more rainwater which infiltrates the soil that is pumped by the plants' roots and contributes to more rainwater leaving the catchment through evapotranspiration while leaving less water that travels through the soil column and leaks into the groundwater in summer compared to winter.
However, it is important to notice that the results showed that a major difference in the partitioning of rainfall between the opposed seasons only occurs if there is enough vegetation inside the catchment. Indeed, in all urban fabric types where there are more than 35% vegetated areas, surface runoff represented the major output flux for rainfall in winter while the evapotranspiration flux represented the main output flux in summer. Instead, in the Industry (the only urban fabric type with less than 30% of vegetated areas), even if the fraction of rainwater leaving the system as surface runoff decreased considerably from winter to summer, surface runoff remained the main output flux for rainfall in both seasons.

The transit time of rainfall inside an urban catchment is also affected by the season of the rainfall event. Indeed, summer rainfall resides less time inside the catchment compared to winter rainfall as the results showed. This can come as a surprise given that in winter most of the rain leaves the catchment immediately as surface runoff whilst in summer much less water goes into surface runoff.
However, in summer, a big part of rainfall gets partitioned into evapotranspiration and the evaporation of water parcels ponding on the soil's surface also starts almost immediately as the travel time distribution curves showed. Moreover, the travel time distribution curves for the evapotranspiration flux also showed that the water parcels move faster in summer compared to winter due to an increase in the evaporation rate due to the hotter temperatures. Thus, there is a higher portion of summer rainfall leaving the urban catchment during the rain event itself and immediately after.
Furthermore, in winter there is more water which leaves the catchment through leakage compared to summer. And, it takes a long time for rainwater to travel through the soil and exit as groundwater recharge as the travel time distribution curve of leakage has shown. Indeed, water going into leakage has a much higher travel time compared to water going into evapotranspiration and surface runoff. Moreover, even if the water parcels going into leakage do move a little faster in winter compared to summer which the travel time distribution curves also showed, the difference in velocity is not enough to compensate for the relative travel time of leakage compared to the other output fluxes. Thus, as there is more water partitioned into leakage in winter, the transit time of winter rainfall on a medium timescale is higher than that of summer rainfall.

The results show that the partitioning of rainfall water inside the urban catchments has a direct influence on the transit time of rainfall inside the catchment. Therefore, since the partitioning of water is very different between seasons, the transit time of rainfall also varies depending on the season during which the rainfall event occurs.

4.2 What are the effects of permeable urban soils on the partitioning and transit time of rainfall water?

The results show that partitioning of rainfall can be heavily affected by the type of landcovers composing a catchment. Indeed, as the proportion of permeable areas increases inside each of the urban fabric types, the fraction of rainfall exiting the catchment through surface runoff decreases while the fraction of rainwater going into evapotranspiration and leakage increases, independently of the season. Therefore, both changes in landcover introducing more permeable surfaces in the conservative scenario and in the radical scenario, if implemented, allow to reduce the amount of rainfall leaving each urban catchment immediately without interacting with it.
However, only when more radical changes are made for each urban fabric type is the partitioning of rainfall really changed and the fraction of rainwater going into surface runoff significantly reduced independently of the season. Indeed, when the maximum amount of permeable surfaces and vegetated surfaces possible are introduced inside each catchment, less than half of the rainwater leaves the system as surface runoff in both seasons without even interacting with it. Therefore, only when enough changes are made which lead to most of the surfaces inside the catchment to be permeable can most of the rainfall infiltrate into the soil and really interact with the system.
Moreover, transforming sealed surfaces into permeable surfaces having no vegetation on them such as gravel in the radical scenario, allows to change the partitioning of infiltrated rainfall. Indeed, increasing the amount of gravel surfaces allows to redirect a bigger part of the rainfall infiltrating the soil into leakage instead of evapotranspiration, especially in winter.

The results also show that the transit time of rainfall inside an urban catchment is dependent on the amount of permeable surfaces that form the overall landcover. Indeed, an increase in permeable areas inside a catchment decreases the amount of rainfall leaving the catchment right after the rain event. This is due to the fact, as seen before, that the amount of surface runoff decreases inside the catchment if the amount of permeable areas increases in either season. Therefore, both conservative landcover changes and radical changes lead to a increase in the transit time of rainfall in the first months that follow the rainfall event.
However, the results show that only if the changes in landcover include a big increase of non vegetated permeable surfaces can the amount of rainfall exiting the catchment in the long term (after one year) for either season decrease. In other words, the overall transit time of rainfall inside each of the different urban fabric types only increases with a significant increase of non vegetated surfaces.
Indeed, increasing the amount of non vegetated surfaces inside the catchment (such as gravel), allows to increase the amount of rainfall going into leakage which takes a very long time to drive water out of the system, while instead, an increase in vegetated surfaces leads to an increase of the rainfall partitioned into evapotranspiration which takes the water out of the system in the 6 months that follow the rain event. Thus, even if the velocity of the water parcels going into evapotranspiration decreases with an increase in the amount of permeable surfaces while the velocity of water parcels going into leakage increases with the increase in permeable surface, the travel time of water parcels going into evapotranspiration is so much shorter than for leakage that a little increase in evapotranspiration leads to rainfall to leave the catchment faster if not enough water is also diverted into leakage to compensate.
Therefore, as only the changes made in the radical scenario allow to considerably increase the fraction of rainfall going into leakage, they are also the only changes which allow to increase the overall transit time of rainfall in all urban fabric types while the landcover changes applied in the conservative scenario only lead to a decrease of the amount of water exiting the catchment right after the rainfall event and thus decrease transit time of water in the month that follows each rainfall event.
However, for an urban fabric type which is in great majority covered in sealed surfaces (asphalt, pavement and building) such as the Industry, even a small increase in permeable areas inside the catchment leads to an increase of the overall transit time of rainfall. This is due to the fact that the amount of rainfall exiting the catchment as surface runoff decreases more than what is gained in rainfall exiting as evapotranspiration by the vegetated surfaces which replace the before 'sealed' surfaces in the conservative scenario.

Overall the results show that the proportions of sealed and permeable surfaces can be modified for the different urban fabric types to change the partitioning and overall transit time of rainfall as they are inherently linked. However, only significant and smart changes in landcover can make a difference and change the overall partitioning of rainfall and its transit time inside an urban landscape.

4.3 Limitations of the project

The use of an ecohydrological model to simulate urban catchments which is normally used to simulate natural catchments leads to some urban processes being ignored.
Indeed, an urban catchment is inherently more complex than a natural catchment in the amount of constraints that are applied to the different natural cycles. The urban fabric shows a very large number of landcovers which are combined to create an intricate mosaic. Green spaces of different size are found in the middle of the built environment thus creating patches where different processes take place. However, these patches most probably are subject to edge effects affecting the different processes and these are not taken into account in this model.
Moreover, as the urban fabric is so complex, there are interactions between the different landcovers that lead to new processes taking place. Indeed, in an urban environment there can be more complex effects to take into account like heat storage in asphalt or cement surfaces, shading by buildings and wind 'funnelling' between buildings which are not integrated into the ecohydrological model used in this project.
Finally, for the simulations implemented in this project, the real growth cycles for vegetation are not activated. Indeed, the dynamic allocation of carbon isn't activated. However, it's activation would allow for a more accurate quantification of the partitioning of rainfall in different seasons in vegetated areas and thus also lead to a better estimate of the transit time of rainfall inside the different urban catchments.
Therefore, the results of this project only give a first approximation in the quantification of the partitioning of specific rainfall events and their transit time inside urban plots with different configurations.

4.4 Next steps

As a next step, the results of this project could be used to estimate rainfall partitioning and water age at the neighborhood scale (entire Pankow neighborhood in Berlin) by using the four urban fabric types analysed to describe the complete watershed.
Furthermore, the results could also help to compute water age and partitioning of rainfall at the Berlin city scale. However, it would be important to first recognize the other typical urban fabric types which can be found inside the catchment such as parks with fountains, parcels with surface water such as man-made channels or rivers, and specific industrial sites which are know to have a direct effect on the water cycle such as wastewater treatment plants (constant water input source) for example.
Moreover, it would be interesting to dive deeper into the behavior of each individual landcover in terms of rainfall partitioning and water age. This would allow to gain further insights into the effects of particular landcovers on the general urban landscape and its water age dynamics.
Finally, it would be interesting to develop a way to include more characteristics of the urban fabric in the description of the catchments used as input for the simulations. Some improvements could be the explicit integration of the stormwater management system or integrating the results of a model simulating the local wind velocity and direction as it can be affected heavily by buildings or integrating the shadow effect created by buildings. This type of improvements would allow to have results from the simulation which are more similar to reality.

5 Conclusion

The use of 'virtual' tracers inside an ecohydrological model granted the ability to track specific rain events inside different urban catchments. This allowed to quantify partitioning of rainfall at a short time scale and gave an estimation of water age in two different seasons in various typical urban landscapes. Moreover, the implementation of different urban development scenarios revealed the effects permeable urban soils have on the urban water cycle. In particular, this project showed that:

- The transit time of water heavily depends on rainfall partitioning and the velocity of water parcels in each output flux.
- Partitioning of rainfall is very dependent on the season of the rainfall event. Indeed, in winter most water becomes surface runoff while in summer a big fraction leaves the system as evapotranspiration.
- Water flows out of an urban parcel faster in summer than in winter regardless of changes in the partitioning of rainfall induced by landcover changes.
- Conservative changes in landcover, which mostly increase permeable surfaces through the increase in vegetated areas, only have a small impact on the partitioning of rainfall events both in summer and in winter and in general don't allow to slow water down as it leaves the catchment.
- Radical changes in landcover which introduce a lot of diversified permeable surfaces, and not only vegetation, allow to decrease surface runoff enough to let most of the rainwater infiltrate the soil while also increasing groundwater recharge enough compared to evapotranspiration to result in longer transit times of water inside the different urban parcels for rainfall events both in summer and winter.

While this work represents a first proof of concept, future work is needed to establish water age as a standard metric in the evaluation of urban planning strategies and their effects on the water cycle.

References

Diamond, John and Thomas Shanley (Jan. 2003). "Infiltration rate assessment of some major soils". In: *Irish Geography* 36.1. Publisher: Routledge _eprint: https://doi.org/10.1080/00750770309555810, pp. 32–46. ISSN: 0075-0778. DOI: 10.1080/00750770309555810. URL: https://doi.org/10.1080/00750770309555810.

Gillefalk, Mikael et al. (June 2021). "Quantifying the effects of urban green space on water partitioning and ages using an isotope-based ecohydrological model". English. In: *Hydrology and Earth System Sciences* 25.6. Publisher: Copernicus GmbH, pp. 3635–3652. ISSN: 1027-5606. DOI: 10.5194/hess-25-3635-2021. URL: https://hess.copernicus.org/articles/25/3635/2021/ (visited on 03/28/2022).

Gillefalk, Mikael et al. (2022). "Estimates of water partitioning in complex urban landscapes with isotope-aided ecohydrological modelling". In: *Hydrological Processes* 36.3, e14532. DOI: https://doi.org/10.1002/hyp.14532. eprint: https://onlinelibrary.wiley.com/doi/pdf/10.1002/hyp.14532. URL: https://onlinelibrary.wiley.com/doi/abs/10.1002/hyp.14532.

GründachPLUS – Berlin Senate promotes green roofs (2020). en-en. URL: https://smart-city-berlin.de/en/news-list/newsdetail?tx_news_pi1%5C%5Bnews%5C%5D=1155&cHash=6a3cffa01014b9f88cdd936eb20e28cc.

KIT - Drought Affected about 90% of the German Territory (Apr. 2021). en-gb. Archive Location: KIT Publisher: KIT-Webmaster (MP). URL: https://www.kit.edu/kit/english/pi_2018_102_drought-affected-about-90-of-the-german-territory.php.

Kuhlemann, Lena-Marie, Doerthe Tetzlaff, and Chris Soulsby (2020). "Urban water systems under climate stress: An isotopic perspective from Berlin, Germany". en. In: *Hydrological Processes* 34.18, pp. 3758–3776. ISSN: 1099-1085. DOI: 10.1002/hyp.13850. URL: https://onlinelibrary.wiley.com/doi/abs/10.1002/hyp.13850.

Kuppel, Sylvain et al. (July 2018). "EcH$_2$O-iso 1.0: water isotopes and age tracking in a process-based, distributed ecohydrological model". English. In: *Geoscientific Model Development* 11.7. Publisher: Copernicus GmbH, pp. 3045–3069. ISSN: 1991-959X. DOI: 10.5194/gmd-11-3045-2018. URL: https://gmd.copernicus.org/articles/11/3045/2018/.

Maneta, M. P. and N. L. Silverman (2013). "A Spatially Distributed Model to Simulate Water, Energy, and Vegetation Dynamics Using Information from Regional Climate Models". In: *Earth Interactions* 17.11, pp. 1–44. DOI: 10.1175/2012EI000472.1. URL: https://journals.ametsoc.org/view/journals/eint/17/11/2012ei000472.1.xml.

McDonnell, Jeffrey J. and Keith Beven (2014). "Debates—The future of hydrological sciences: A (common) path forward? A call to action aimed at understanding velocities, celerities and residence time distributions of the headwater hydrograph". en. In: *Water Resources Research* 50.6. _eprint: https://onlinelibrary.wiley.com/doi/pdf/10.1002/2013WR015141, pp. 5342–5350. ISSN: 1944-7973. DOI: 10.1002/2013WR015141. URL: https://onlinelibrary.wiley.com/doi/abs/10.1002/2013WR015141.

Zhou, Zhengzheng et al. (2017). "The complexities of urban flood response: Flood frequency analyses for the Charlotte metropolitan region". en. In: *Water Resources Research* 53.8, pp. 7401–7425. ISSN: 1944-7973. DOI: 10.1002/2016WR019997. URL: https://onlinelibrary.wiley.com/doi/abs/10.1002/2016WR019997.

Appendix

	Land cover							
Soil parameters	Asphalt	Building	Grass	Gravel	Pavement	Shrub	Trees	Vegetated roof
Total soil depth [m]	5	5	2.35	5	5	1.2	4.65	2.35
Thickness of first hydrological layer [m]	0.05	0.05	0.1	0.1	0.05	0.25	0.25	0.1
Thickness of second hydrological layer [m]	0.5	0.5	0.5	0.5	0.5	0.5	0.5	0.1
Porosity of first and second hydrological layer [–]	0.1	0.01	0.4	0.2	0.2	0.2	0.45	0.45
Porosity of third hydrological layer [–]	0.3	0.3	0.3	0.3	0.3	0.3	0.3	0.3
Air-entry pressure head [m]	0.3	0.3	0.35	0.3	0.3	0.22	0.39	0.35
Saturated horizontal hydraulic conductivity of first hydrological layer [ms^{-1}]	10^{-9}	10^{-12}	$2x10^{-2}$	10^{-6}	10^{-8}	$2x10^{-2}$	$2x10^{-2}$	$2x10^{-2}$
Saturated horizontal hydraulic conductivity of second hydrological layer [ms^{-1}]	10^{-12}	10^{-12}	$2x10^{-2}$	10^{-6}	10^{-8}	$2x10^{-2}$	$2x10^{-2}$	10^{-12}
Saturated horizontal hydraulic conductivity of third hydrological layer [ms^{-1}]	10^{-3}	10^{-3}	$2x10^{-2}$	10^{-3}	10^{-3}	$2x10^{-2}$	$2x10^{-2}$	$2x10^{-3}$
Brooks–Corey exponent [–]	2.2	2.2	3.0	2.2	2.2	2.3	2.1	3.0
Albedo [-]	0.05	0.1	0.18	0.3	0.1	0.18	0.16	0.18
Ratio of vertical to horizontal hydraulic conductivity [-]	0.4							
Surface emissivity [-]	0.98							
Dry soil heat capacity [$Jm^{-3}K^{-1}$]	$2.5x10^{-6}$							
Dry soil thermal conductivity [$Wm^{-1}K^{-1}$]	0.15							
Damping depth : depth of bottom of second soil thermal layer [m]	2							
Soil temperature at damping depth [°C]	10							
Snow melt coefficient [$m°C^{-1}$]	$4.1x10^{-8}$							
Soil bedrock leakance [-]	0.5							
Local surface roughness [m]	0.05							
Residual soil moisture [m^3m^{-3}]	0.0009							
Vegetation water use parameter (Wc) [m]	0.7							
Vegetation water use parameter (Wp) [m]	9							

Table A1: List of the soil parameters used to run the simulations. The parameters which are dependent on landcover type for grass, shrub and trees are taken from Gillefalk et al., 2021, the others were estimated from literature at the beginning of the WANH project

In table A1, soil properties are homogeneous through each individual landcover. Indeed, the assumption is made that the soil properties are much more dependent on the landcover type than on the geomorphology of the land. Thus, the spatial hetereogenity of the soil parameters is given solely by the change in landcover between the different pixels.

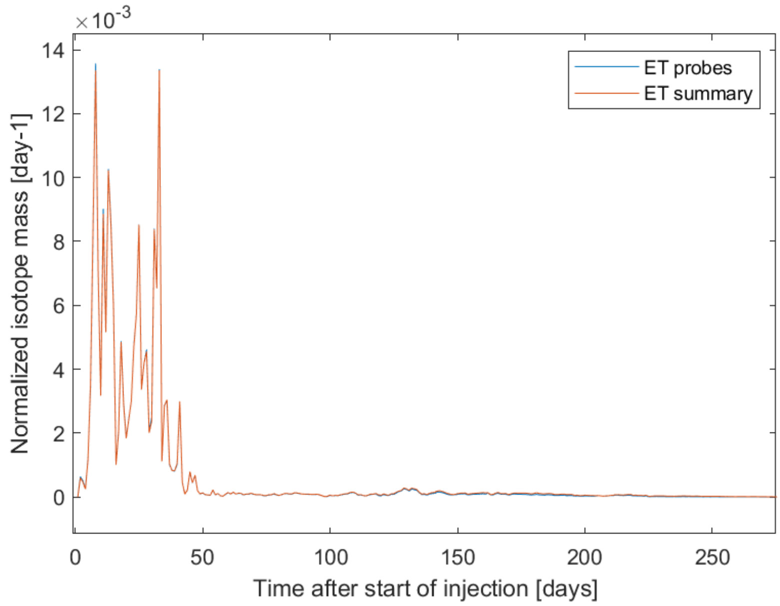

Figure A1: Comparison of the normalized breakthrough curves obtained for the test catchment covered solely with vegetated landcovers. The red curve represents the NMBTC obtained by using timeseries of ET flux and its signature given as outputs of the model. The blue curve represents the NMBTC obtained by using the timeseries of ET flux given as output of the model and the timeseries of isotope signature of the ET flux calculated using the algorithm developed for this project.

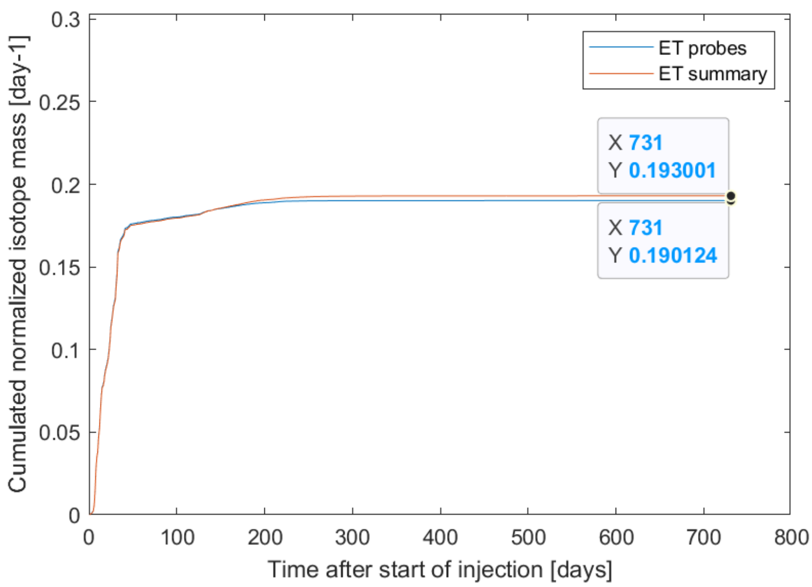

Figure A2: Comparison of the normalized cumulative breakthrough curves obtained for the test catchment covered solely with vegetated landcovers. The red curve represents the cumulative NMBTC obtained by using timeseries of ET flux and its signature given as outputs of the model. The blue curve represents the cumulative NMBTC obtained by using the timeseries of ET flux given as output of the model and the timeseries of isotope signature of the ET flux calculated using the algorithm developed for this project.

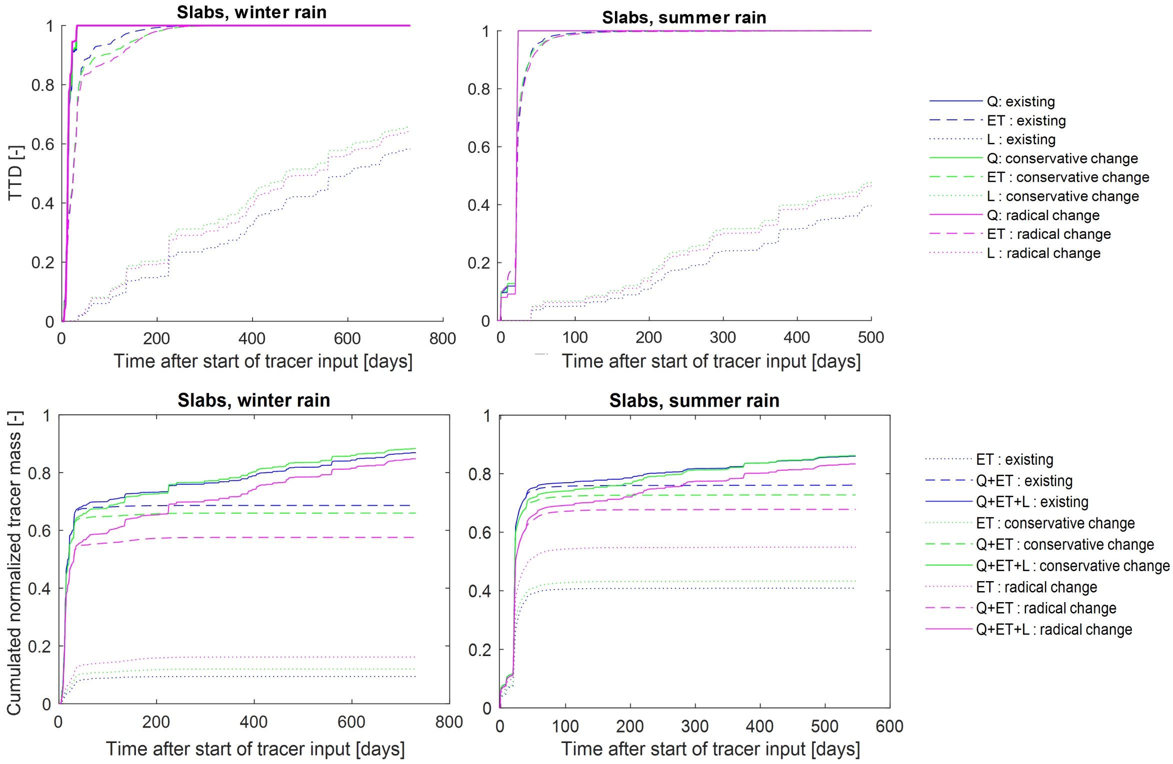

Figure A3: (Top) TTD curves for summer and winter rainfall events in the Slabs. (Bottom) cumulative NMBTC of evapotranspiration, evapotranspiration and surface runoff together and all output fluxes together (ET, Q and L) for summer and winter rainfall events in the Slabs.

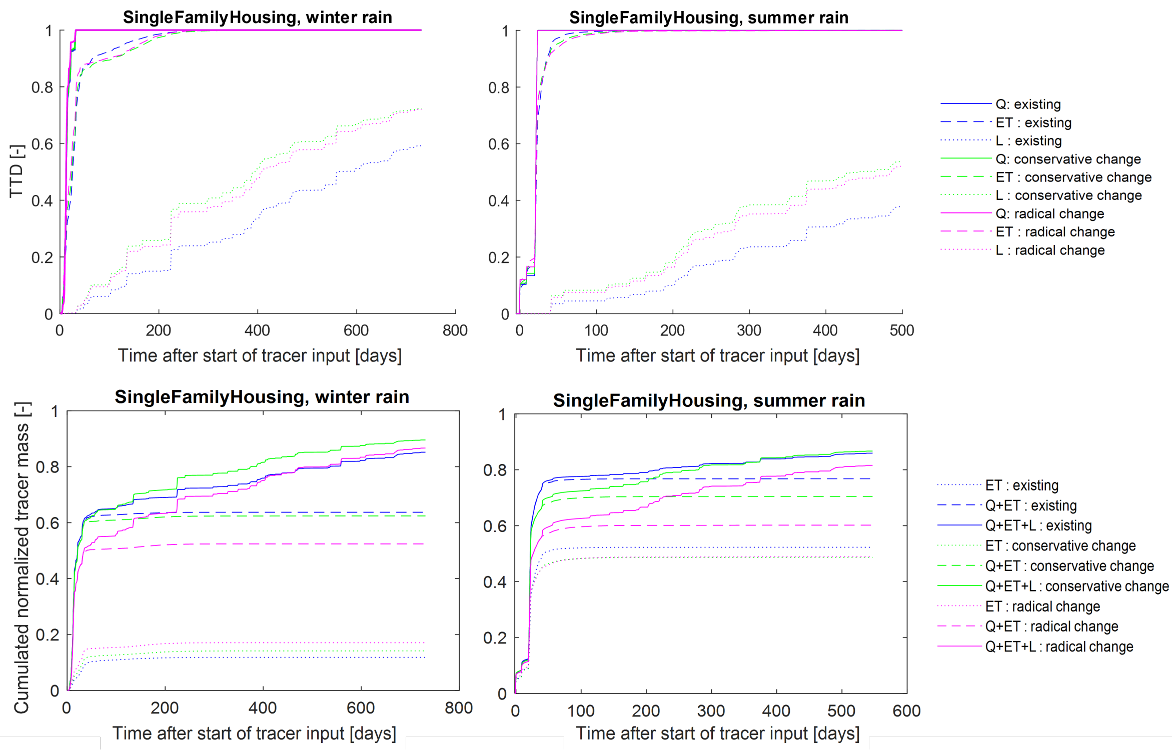

Figure A4: (Top) TTD curves for summer and winter rainfall events in the SingleFamilyHousing. (Bottom) cumulative NMBTC of evapotranspiration, evapotranspiration and surface runoff together and all output fluxes together (ET, Q and L) for summer and winter rainfall events in the SingleFamilyHousing.

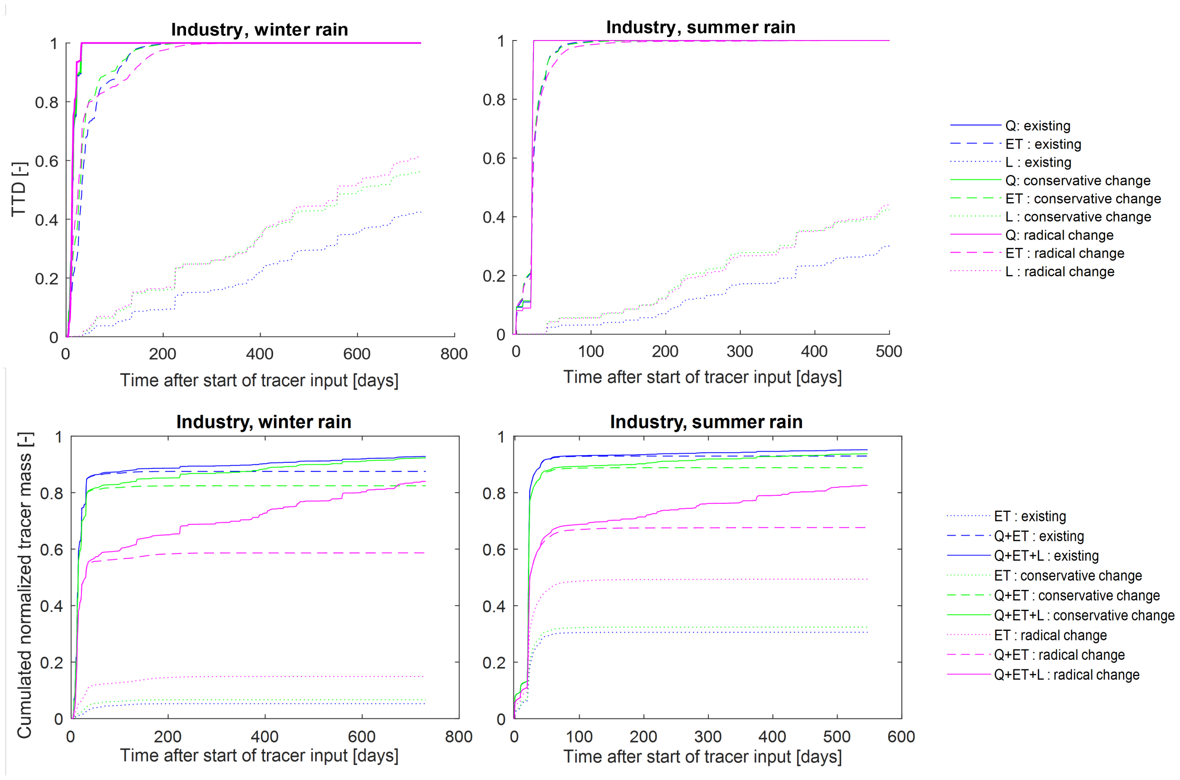

Figure A5: (Top) TTD curves for summer and winter rainfall events in the Industry. (Bottom) cumulative NMBTC of evapotranspiration, evapotranspiration and surface runoff together and all output fluxes together (ET, Q and L) for summer and winter rainfall events in the Industry.